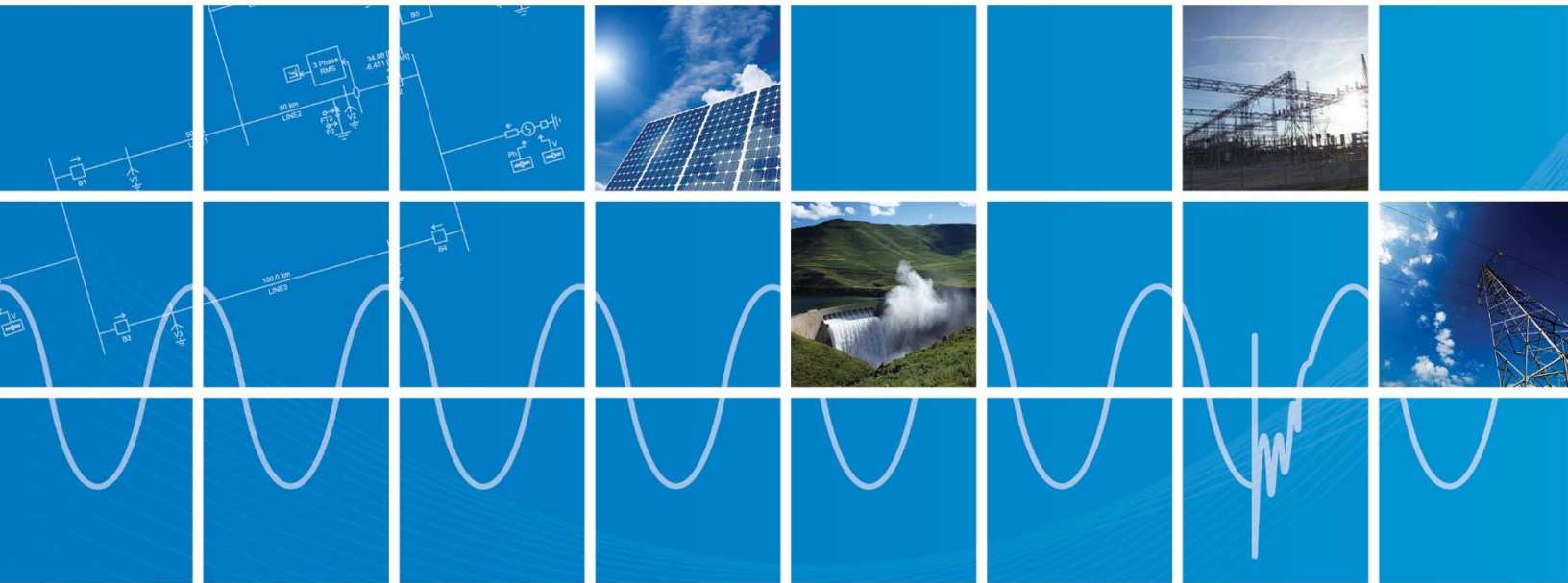


# Type 3 Wind Turbine Model

Written for PSCAD X4 version 4.6

November 21, 2018

Revision 3



Powered by Manitoba Hydro International Ltd.  
211 Commerce Drive  
Winnipeg, Manitoba  
R3P 1A3 Canada  
mhi.ca



## Contents

1	General Description of the Simulation .....	1
2	Electrical and mechanical components of Type-3 wind turbine.....	3
2.1	Wind Turbine and Power Network .....	4
2.2	Mechanical Model.....	6
2.2.1	Turbine .....	6
2.2.2	Wind power model .....	7
2.2.3	Pitch Angle Controller .....	10
2.3	Electrical Model.....	11
2.3.1	AC-DC-AC Converters.....	12
2.3.2	AC-DC-AC Converters parameters .....	13
2.3.3	Detailed Converter Model .....	17
2.3.4	Average Converter Model.....	18
2.3.5	Grid-side controller .....	19
2.3.6	Rotor-side controller.....	23
2.4	Start-up Sequence of the Electrical System .....	27
2.4.1	Synchronization .....	29
2.5	Crowbar Protection .....	30
2.6	DC-link Chopper .....	32
2.7	Low Pass Filter .....	33
2.7.1	Filter parameters calculation .....	34
2.8	Scaling Component .....	36
3	Dynamic responses of the detailed and the average models .....	37
3.1	Dynamics against wind speed variations .....	37
3.2	Dynamics against faulty condition .....	39
4	References .....	41

---

## 1 General Description of the Simulation

Load the work space (i.e. Type3WindTurbine.pscx) into PSCAD. The workspace is similar to what is shown in Figure 1 with the name of the simulation and the hierarchy tree of the modules.

The simulation case Type3\_Dlt\_Nov\_2018 contains of the detailed model of the wind turbine and the case Type3\_Ave\_Nov\_2018 consists of its average model. The hierarchy tree is useful to realise what are the active modules in the simulation and navigate through them easily. As can be seen in the main canvas there are three custom modules: TLine, Cable\_1 and Type3\_WTG\_Dtl. Click on + to expand the hierarchy tree to see the submodules.

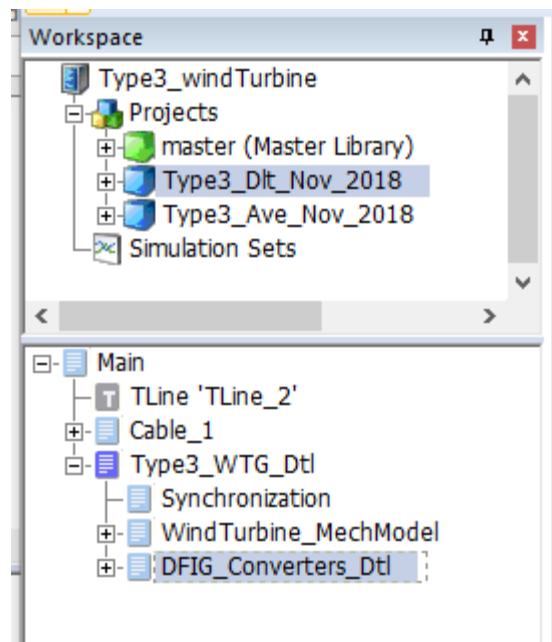


Figure 1: Workspace and hierarchy tree of modules

Click on the module named DFIG\_Converters\_Dtl to see the converter circuit for the detailed model shown in Figure 2.

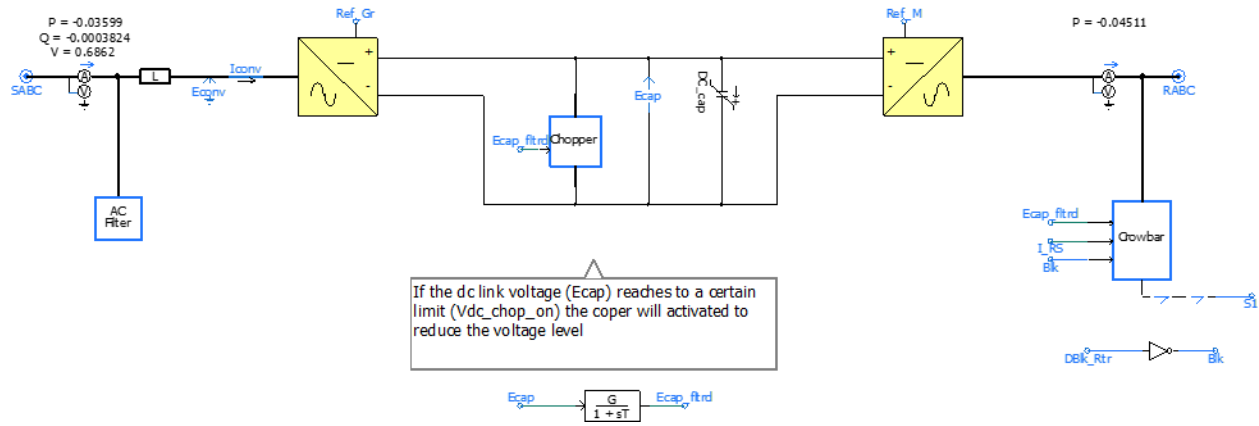


Figure 2: Type-3 wind turbine with detailed converter model

Note: The detailed model consists of insulated-gate bipolar transistor (IGBT) switches therefore harmonics and transient behaviors related to switching can be modeled accurately. However, a small solution time step is unavoidable to properly simulate the IGBT switching which increases the simulation time.

Same process can be done for the Type3\_Ave\_Nov\_2018 to see the Workspace and hierarchy tree of modules as shown in Figure 3.

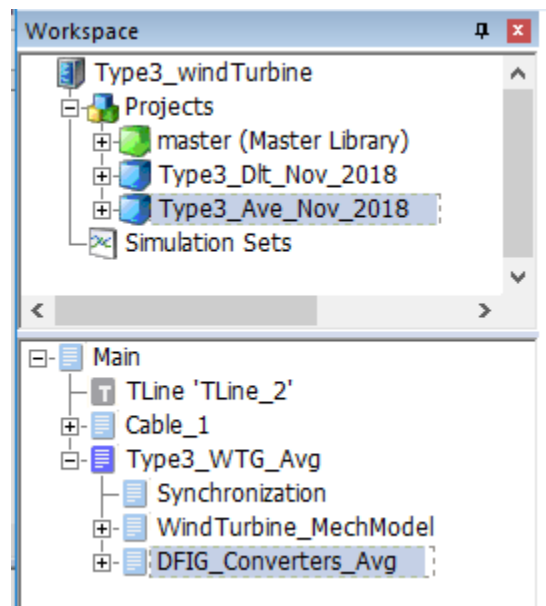


Figure 3: Workspace and hierarchy tree of modules

Also click on the module named DFIG\_Converters\_Avg to see the converter circuit for the average model shown in Figure 4.

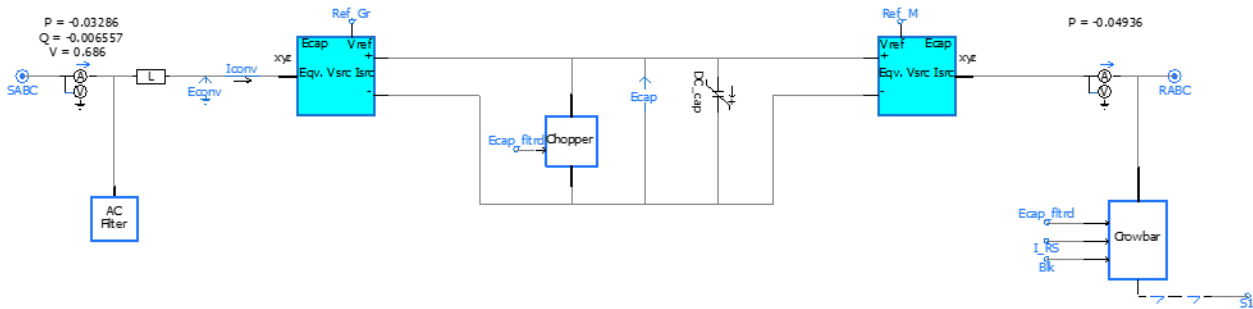


Figure 4: the Type-3 wind turbine with average converter model

Note: The average model of the converter consists of equivalent current and voltage sources. This model does not require switching (i.e. non-switching) therefore the solution time step can be increased significantly compared to the detailed one. This saves significant simulation time; however, transient behavior of the converter and harmonics maybe not be fully represented during simulations. This model may be used for particular power system studies where slow transients are of interest, and for most fault ride through cases [1].

Note: From now on what will be explained for the wind turbine is true for both detailed and average models unless otherwise it is clearly emphasised. Nevertheless, the only difference between the average and detailed model is in the converter model as stated clearly in this section.

## 2 Electrical and mechanical components of Type-3 wind turbine

Type-3 wind turbine generator (WTG) also known as Doubly-Fed Induction Generator (DFIG) is presented in this section. It is described in the form of two separate systems - mechanical and electrical – as shown in Figure 5. The mechanical system extracts the maximum available power from the wind and yields mechanical torque. The electrical system, converts the mechanical torque to the electrical one and thus electric power. The interface between mechanical and electrical systems is the induction machine (IM), which converts the mechanical energy into electrical energy. The mechanical and electrical systems shown in Figure 5 are represented by the following components.

1. Mechanical System consists of (described in Section 2.2):
  - i. Wind Turbine
  - ii. Pitch Angle Controller
2. Electrical system consists of (described in Section 2.3):
  - i. Grid-side Converter and Controls
  - ii. Rotor-side Converter and Controls
  - iii. DC-link Chopper Protection
  - iv. Crowbar Protection
  - v. Low Pass Filter

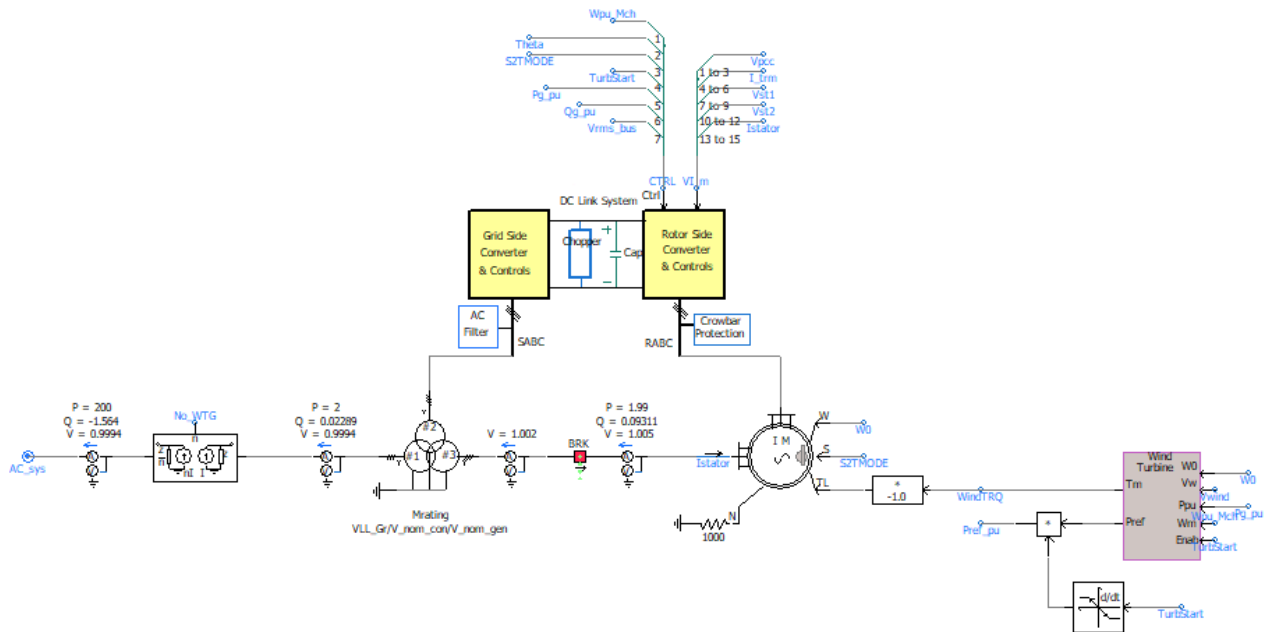
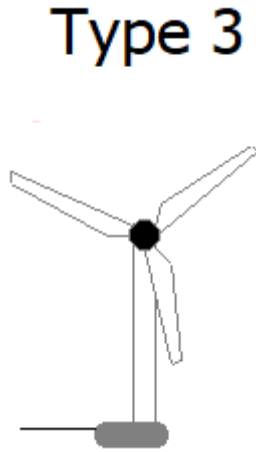


Figure 5: Electromechanical system of wind turbine for both average and detailed models

## 2.1 Wind Turbine and Power Network

Figure 6 shows the Type-3 wind turbine (WT) component and its input parameters. These parameters are the same for both average and detailed model. The parameters can be seen by a right click on the component and selecting Edith Parameters.



(a)

Configuration	
<b>1. General</b>	
Enable/Disable the wind turbine	Dblk
Nominal system frequency	freq
AC voltage magnitude	Vbase
Total number of wind turbine generator	UN
DFIG rated active power at HV terminals [MW]	Rated_MW
Input wind speed	Vwind
Cut-in wind speed	3.0 [m/s]
Cut-out wind speed	25.0 [m/s]
<b>2. Induction Machine parameters</b>	
Machine MVA rating	Machine_MVA
Machine base angular frequency [rad/s]	376.99112
Maximum operating slip of induction machine	0.3
<b>3. Mechanical parameters</b>	
Turbine RPM at machine nom speed	12 [rpm]
Nominal wind speed	11 [m/s]

(b)

Figure 6: Type-3 wind turbine for both average and detailed models (a) the wind turbine component (b) the input parameters

Table 2 shows the caption, type, unit and value for all the input parameters. The properties can be seen by a right click on the component and selecting View Properties. This View Properties helps to see the parameters name in the simulation and clarify other important information about them.

Table 1: Input parameters of the Type-3 wind turbine model

NAME	CAPTION	TYPE	UNIT	VALUE
Dblk	Enable/Disable the wind turbine	Real	-	Dblk
freq	Nominal system frequency	Real	Hz	freq
VLL_Gr	AC voltage magnitude	Real	kV	Vbase
No_WTG	Total number of wind turbine generator	Real	-	UN
Pbase	DFIG rated active power at HV terminals [MW]	Real	MW	Rated_MW
VRot_nom	Turbine RPM at machine nom speed	Real	rpm	12
Vwind	Input wind speed	Real	m/s	Vwind
Mrating	Machine MVA rating	Real	MVA	Machine_MVA
OMEG	Machine base angular frequency [rad/s]	Real	rad/s	376.99112
Vw_nom	Nominal wind speed	Real	m/s	11
Slip_max	Maximum operating slip of induction machine	Real	-	0.3
vWcutin	Cut-in wind speed	Real	m/s	3
vWcutout	Cut-out wind speed	Real	m/s	25

Figure 7 shows the overall power system in which a wind turbine Type-3 (detailed or average) is connected to the power network via a cable, transformer and transmission line. The short circuit ratio of at the terminal of the wind turbine is 1.8.

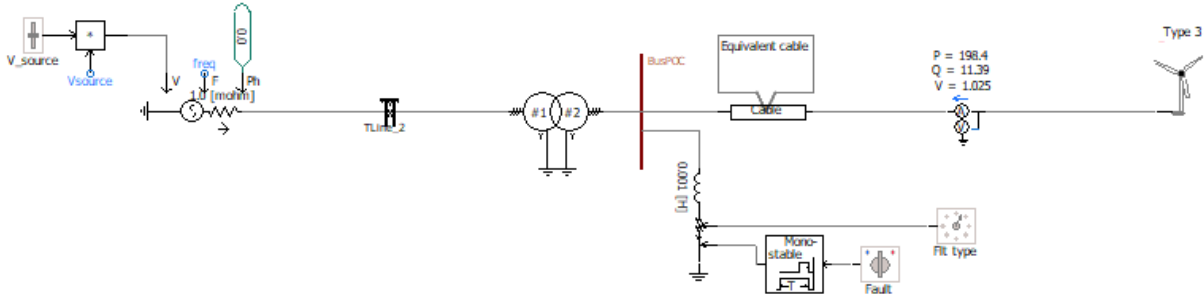


Figure 7: Overall power system with Type-3 wind turbine (WT) and equivalent current source

## 2.2 Mechanical Model

### 2.2.1 Turbine

The wind turbine component shown in Figure 8 models the mechanical dynamics and pitch controller. The main function of the wind turbine is to extract maximum power from available wind without exceeding the rating of the equipment. Some limitations exist at zero-power operation – when the wind speed is lower than 4 m/s, and when there is excessive wind, with wind speeds higher than 25m/sec. The nominal wind speed is 11m/s.

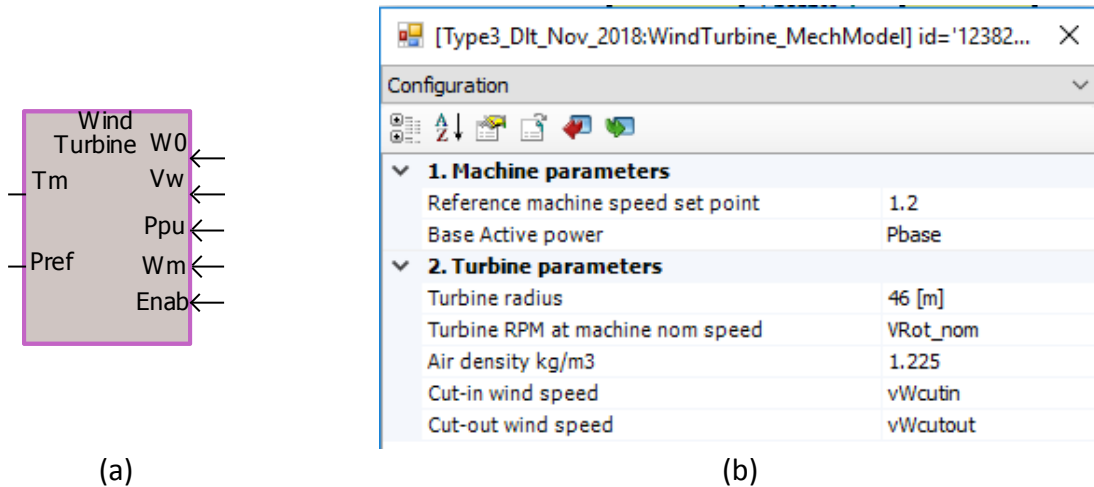


Figure 8: Wind turbine model: (a) the component and (b) its parameters



Table 2 lists the View Properties of the input and output parameters of the wind turbine component.

The properties can be seen from a right click on the component and select View Properties.

Table 2: Input/output signals of the wind turbine model

Rad_turb	Turbine radius	Real	m	46 [m]	46
Wref_sp	Reference machine speed set point	Real	pu	1.2	1.2
VRot_nom	Turbine RPM at machine nom speed	Real	rpm	VRot_nom	VRot_nom
rho	Air density kg/m <sup>3</sup>	Real		1.225	1.225
Pbase	Base Active power	Real	MW	Pbase	Pbase
vWcutin	Cut-in wind speed	Real	m/s	vWcutin	vWcutin
vWcutout	Cut-out wind speed	Real	m/s	vWcutout	vWcutout

### 2.2.2 Wind power model

The mechanical power of wind turbine obtained from the wind energy can be calculated based on the following formula [1]:

$$P = \frac{\rho}{2} \times A_r \times V_W^3 \times C_p(\lambda, \theta) \quad (1)$$

Where

$P$ : mechanical power extracted from the wind turbine;

$\rho$ : air density in  $\frac{kg}{m^3}$ ;

$A_r$ : area swept by the rotor blades in  $m^2$ ;

$V_W$ : wind speed in  $\frac{m}{sec}$ ;

$\lambda$ : tip speed ratio

$\theta$ : pitch angle

$C_p$ : power coefficient, which is function of  $\lambda$  and  $\theta$ .

$C_p$  is a characteristic of the wind turbine that is usually provided by the manufacturer as a set of curves relating  $C_p$  to  $\lambda$  with  $\theta$  parameters.

The PSCAD implementation of  $\lambda$  is shown in Figure 9.

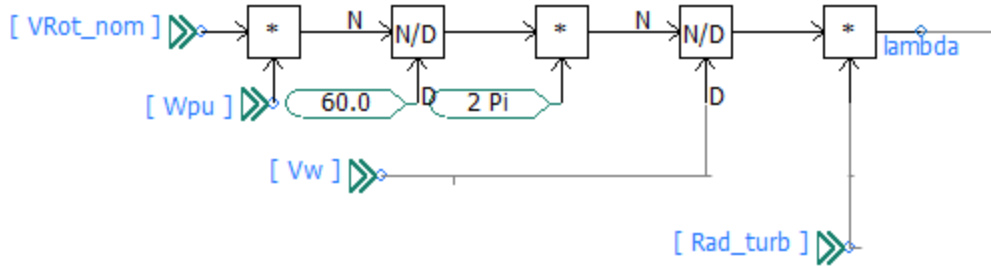


Figure 9: Tip-speed ratio calculation

The calculation of the power coefficient used in this example follows the  $C_p$  curves provided in [2]. The  $C_p$  calculation is given in terms of a fourth order polynomial of the following form:

$$C_p(\theta, \lambda) = \sum_{i=0}^4 \sum_{j=0}^4 (\alpha_{i,j} \cdot \theta^i \cdot \lambda^j) \tag{2}$$

The curve gives a good approximation for values of  $3 < \lambda < 15$  and negative  $C_p$  are limited to  $-0.05$ . The  $\alpha_{i,j}$  can be represented as a 5x5 matrix using 25 coefficients, as shown in Figure 10.

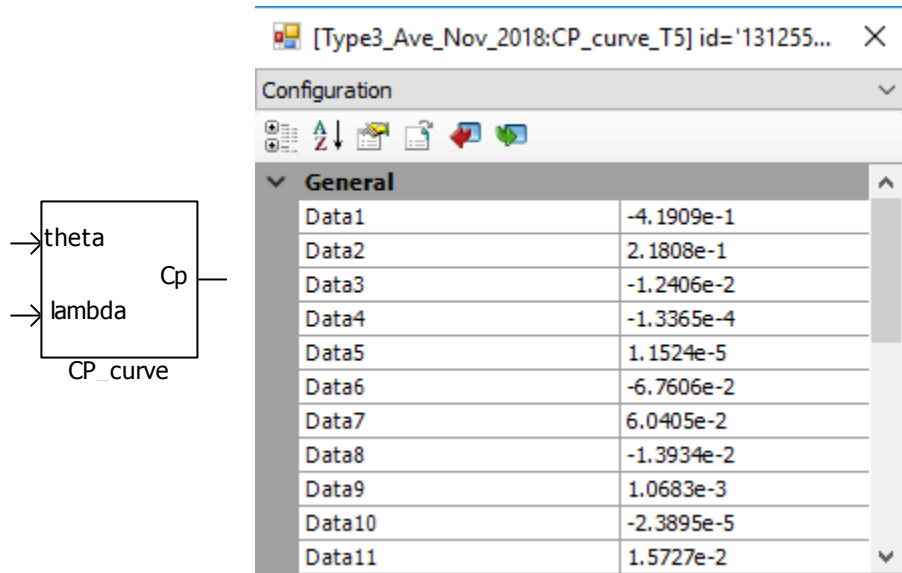


Figure 10: Look up table for polynomial function of  $C_p$

An alternative approach to obtain  $C_p$  is also provided in the turbine mechanical model:

$$C_p(\theta, \lambda) = C_1 \left( \frac{C_2}{\lambda_i} - C_3\theta - C_4 \right) e^{-\frac{C_5}{\lambda_i}} + C_6 \cdot \lambda \tag{3}$$

with  $\frac{1}{\lambda_i} = \frac{1}{\lambda + 0.08\theta} - \frac{0.035}{\theta^3 + 1}$

and  $C = [0.5176, 116, 0.4, 5, 21, 0.0068]$

The results of modelling of power coefficient i.e.  $C_p$  based on polynomial approximation represented in (3) and functional represented in (4) are shown in Figure 11 for 0, 5 and 25 degrees of pitch angle.

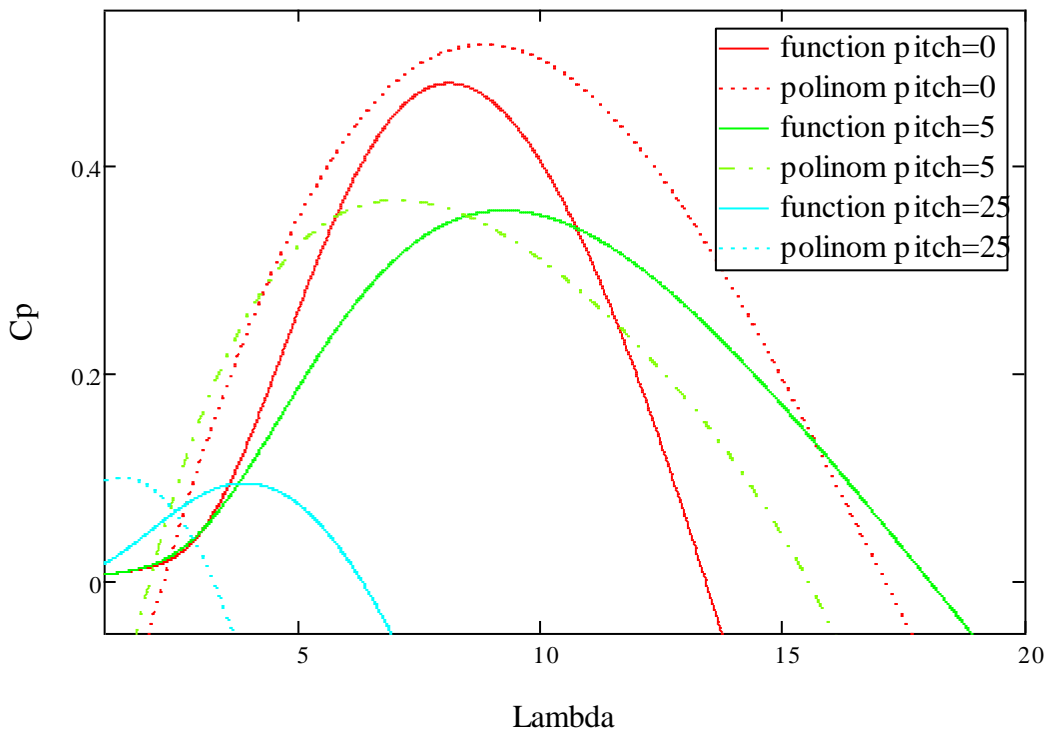


Figure 11: Power coefficient as function of pitch angle and tip-speed

The maximum power point tracing is obtained as follows (see the reference [4] equation (16)):

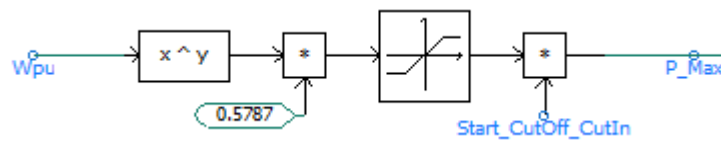


Figure 12: Maximum power point tracking based on the mechanical speed

The overall aerodynamic model of the wind turbine implemented for both average and detailed models is shown in Figure 13.

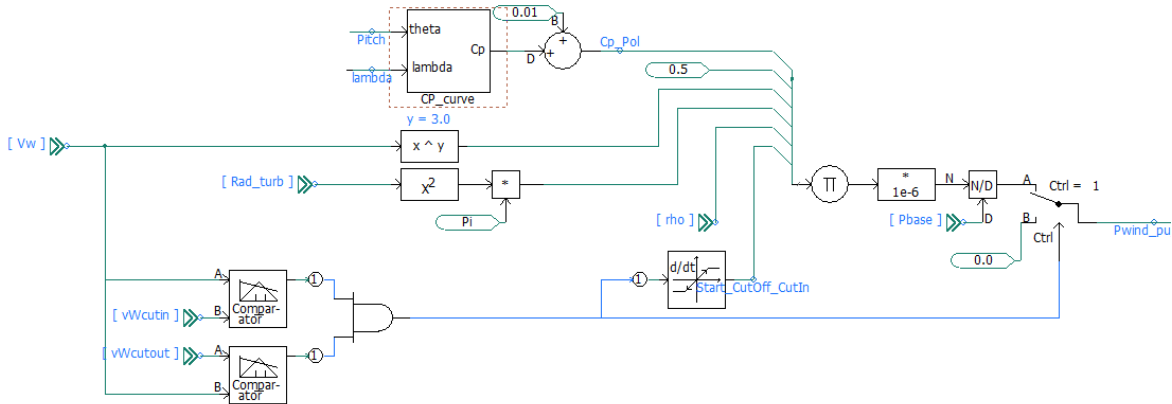


Figure 13: Mechanical power implementation of the wind turbine

### 2.2.3 Pitch Angle Controller

When the wind speed exceeds the rated speed, the available mechanical power exceeds the rated power of the induction machine. The power delivered to the electrical system is limited by reducing the effective area of the blade. This is achieved by increasing the pitch angle. A typical range for the pitch angle is between 0° and 25°. The controller loop for pitch angle determination is represented in Figure 14.

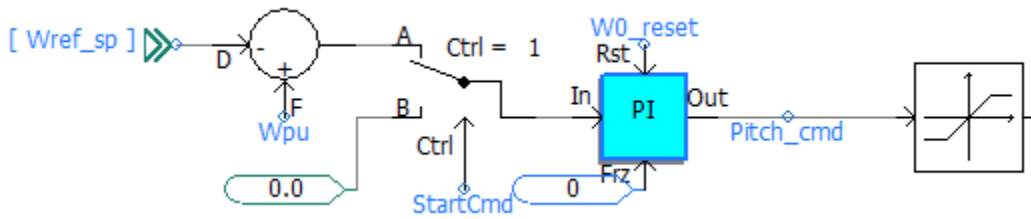


Figure 14: simplified pitch angle controller

As shown in Figure 14, the pitch controller defines high ( $vW_{cutout}$ ) and low ( $vW_{cutin}$ ) wind speeds for the turbine. Outside this range the pitch angle controller is frozen and power is set to zero.

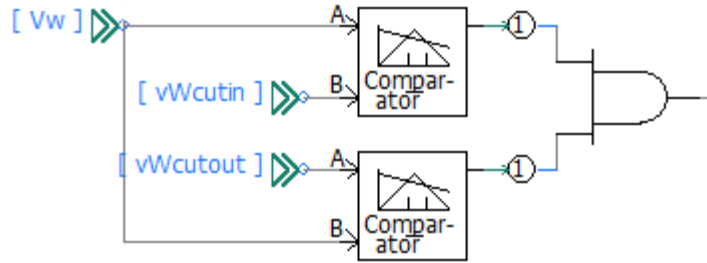
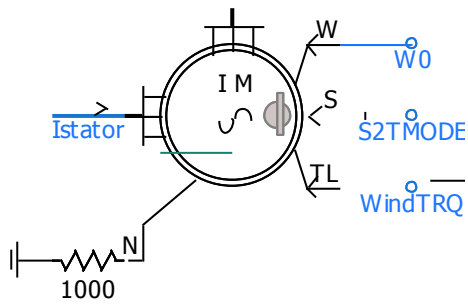


Figure 15: Pitch angle limitation.

### 2.3 Electrical Model

In this document the electrical part of the wind turbine is consist of indication machine and the AC-DC-AC converter. This document mostly describes the converter and its associations.

Figure 16 shows the induction machine and its terminal descriptions. The induction machine is started in speed control mode as the input 'S' is set to 1. The value in input 'W' with the speed of the machine set to a preselected value  $\omega_0$ . Ideally this speed should be setup close to the final steady state rotating speed which is 1.2 pu. When the induction machine is synchronized with the grid the S turns to zero and it operates at torque control mode.



(a)

(b)

Figure 16: PSCAD Wound rotor machine component: terminal descriptions

- W: Speed input in per-unit. When machine is in speed control mode the machine runs at W0 speed.
- S: A switch to select speed control mode (1) or torque control mode (0).
- T: Torque input in per-unit. If the machine is in torque control mode then the machine computes the speed based on the inertia and damping coefficient, the input and output torques

### 2.3.1 AC-DC-AC Converters

The AC-DC-AC converter is shown in Figure 17. The AC-DC-AC converter consists of:

- Rotor-side converter,
- Grid-side converter,
- DC-link system,
- Grid-side Control, and
- Rotor-side Control.

Also in Figure 17 the other important parts of the system are;

- Crowbar protection,
- DC-link chopper, and
- Low pass filter.

The grid-side converter controls the DC voltage and, while the rotor-side converter controls active power and AC voltage by controlling the currents of the rotor circuit. In this example both converters, rotor- and grid-side, operate as Voltage Source Converters (VSC).

1. Note that the rotor-side converter and grid-side converter are modeled as detailed and average model and described in the sections 5.1.2 and 5.1.3 respectively.

2. The grid-side and rotor-side controllers, described in the sections 5.1.4 and 5.1.5 respectively are applied to both detailed and average models.
3. The crow-bar circuit is used to protect the rotor-side converter against high current induced from stator into rotor during fault events.
4. The DC chopper is used to protect the DC bus from over voltages and the A more detailed description of these devices is provided in subsequent sections.
5. An AC filter is used on the grid-side converter side to remove some of the voltage harmonics of the two-level converter.

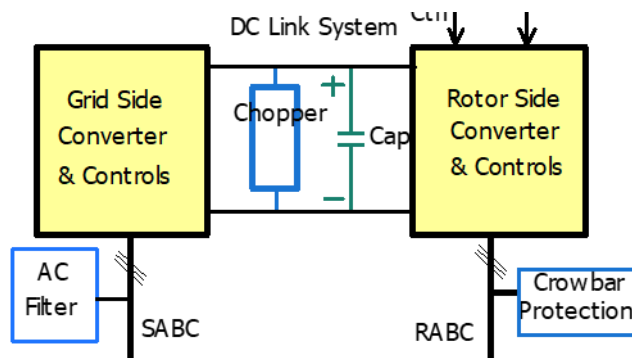


Figure 17: AC-DC-AC converter consists of grid-side, rotor-side converters, chopper, DC-Link, crowbar protection and low-pass filter.

### 2.3.2 AC-DC-AC Converters parameters

This section describes the parameters of the AC-DC-AC converters in Table 3, Table 4 and Table 5. To see the parameters right click on the component and select “Edit parameters”. Those parameters in tabled that have a signal name as their value can be modified by sliders. Some of these sliders are shown in Figure 18.

Table 3: AC-DC-AC Converters parameters

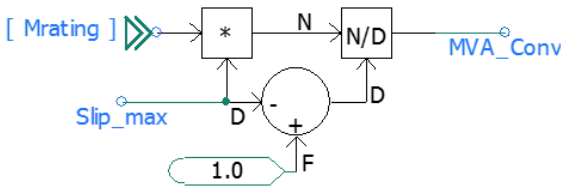
Parameter	Value	Description
<b>1. General</b>		
Capacitance	7200 [ $\mu$ F]	DC bus capacitance
AC system frequency	freq	Nominal AC system frequency
Voltage on high side of TRF	VLL_Gr	Voltage of the Wind Farm collector system
<b>2. Machine parameters<sup>1</sup></b>		
System MW at PCC	Pbase	The expected full active power at the point of common coupling. This value is used as the base active power 'Pbase' for per-unitization of quantities
Machine rating	Mrating	The MVA rating of the machine.
Machine terminal voltage	V_nom_gen	Nominal voltage of the stator terminals
Stator resistance	Rs_pu	Per unit value of the resistance of the stator windings
Slip_max	Slip_max	Maximum operating slip of the machine
Stator/Rotor turns ratio	TRNR	Turns ratio between stator and rotor windings
<b>3. Filter parameters</b>		
Filter Calculation	1	1: uses a generic calculation shown in Appendix 1. 0: uses the RLC values entered below.
Cutoff frequency	300 [Hz]	Cutoff frequency for the low pass filter
Cfilter	300 [ $\mu$ F]	Main filter capacitance
Cdamp	350 [ $\mu$ F]	Damping branch capacitance
Ldamp	621 [ $\mu$ H]	Damping branch inductance
Rdamp	1.332[ohm]	Filter's damping resistance
<b>4. DC chopper</b>		
Activation voltage	1.654 [kV]	Chopper hysteresis control activation voltage
Off voltage	1.605 [kV]	Chopper hysteresis control turn off voltage
Shunt resistor	0.98 [ohm]	Chopper resistance
<b>5. Crowbar protection</b>		
Crowbar enable	Crow_Enab	Crowbar enabled (1), disabled (0)
DC crowbar on voltage	1.75 [kV]	Crowbar activation by DC link overvoltage: Activation voltage
Maximum Irotor	Icrow_bar	Crowbar activation by overcurrent in rotor circuit: Activation current
Activation time	Tcrow_bar	This time is the duration of crowbar activation
Crowbar resistance	0.001 [ohm]	series resistance of the crowbar system
Crowbar inductance	40 [ $\mu$ H]	series inductance of the crowbar system



Table 4: DFIG Converters page parameters: Grid-side Converter (GSC)

Parameter	Value	Description
<b>1. General</b>		
De-block signal	-	A signal should be provided here to indicate when the converter de-blocks. (0:blocked, 1:de-blocked). When initializing the simulation, this transition should happen before the rotor side converter is de-blocked
Rated MVA	MVA_Conv	Rating of the grid side converter in MVA. Typically between 20 and 40% of the Wind Turbine Generator rating (see eq (6))
Rated AC voltage	0.69 [kV]	Voltage on the AC side of the grid-side converter
Vdc base	1.45 [kV]	Base DC voltage of DC bus
DC voltage order	Edc_ord	DC voltage order in kV
Reactive power order	Q_ord	Reactive power order in MVAR
Current controller upper limit order	1.2 [pu]	Maximum current allowed in converter compared to nominal current at nominal voltage
Converter VSC reactor	192 [uH]	VSC reactor for grid-side Converter
Carrier frequency multiple	60	Carrier frequency expressed as a multiple of the fundamental frequency
<b>2. d-axis control (Real power axis)</b>		
d regulator gain	KpdS	d-axis PI controller proportional gain
d regulator time constant	TidS	d-axis PI controller time constant
<b>3. q-axis control (Reactive power axis)</b>		
q regulator gain	KpqS	d-axis PI controller proportional gain
q regulator time constant	TiqS	d-axis PI controller time constant
<b>4. DC voltage control</b>		
Edc regulator gain	Kp_Edc	DC voltage PI controller proportional gain
Edc regulator time constant	Ti_Edc	DC voltage PI controller time constant
<b>5. Reactive power control</b>		
Q regulator gain	Kp_Q_S	Reactive power PI controller proportional gain
Q regulator time constant	Ti_Q_S	Reactive power PI controller time constant
<b>6. PLL control</b>		
PLL time constant	Ki_PLL_Gr	Grid side converter PLL integral gain
PLL gain	Kp_PLL_Gr	Grid side converter PLL proportional gain

The rating of the grid-side and rotor-side converters is estimated in terms of the maximum operating slip (see equation (15) in the reference [3]):



$$MVA\_Conv = \frac{Mrating \cdot Slip\_max}{1.0 + F - D} \quad (4)$$

where  $slip\_max$  is the maximum operating slip and  $Mrating$  is the WTG MVA rating.

Table 5: DFIG Converters page parameters: Rotor-Side Converter (RSC)

Parameter	Value	Description
<b>1. General</b>		
q axis control mode	0	Define the mode of control for rotor-side controller. q axis control mode (0: Q control 1: Vac control)
De-block signal	DBlk_Rsc	A signal should be provided here to indicate when the converter de-blocks. (0:blocked, 1:de-blocked). When initializing the simulation, this transition should happen after the grid side converter is de-blocked
Rated MVA	MVA_Conv	Rating of the grid side converter in MVA. Typically between 20 and 40% of the Wind Turbine Generator rating
RatedAC voltage	0.69 [kV]	Voltage on the AC side of the grid-side converter
Active power order	Pref_pu	Reactive power order in MVAR
Reactive power order	Qref_pu	Reactive power order in MVAR
Current controller upper limit order	1.2 [pu]	Maximum current allowed in converter compared to nominal current at nominal voltage
Carrier frequency multiple	37	Carrier frequency expressed as a multiple of the fundamental frequency
<b>2. d-axis control for start-up</b>		
Kpd_st (startup)	Kpd_st	d-axis PI controller proportional gain to be used in the pre-synchronization phase during start-up
Tid_st (startup)	Tid_st	d-axis PI controller time constant to be used in the pre-synchronization phase during start-up
<b>3. d-axis control (Active power axis)</b>		
Kpd_R	Kpd_R	d-axis PI controller proportional gain to be used in the inner PI controller
Tid_R	Tid_R	d-axis PI controller time constant to be used in the inner PI controller
KpP_PCC	KpP_PCC	d-axis PI controller proportional gain to be used in the PCC active power PI controller. Note that the order for this controller is iPCmd provided by the IEC control blocks
TiP_PCC	TiP_PCC	d-axis PI controller time constant to be used in the PCC active power PI controller. Note that the order for this controller is iPCmd provided by the IEC control blocks
<b>4. q-axis control (Reactive power axis)</b>		

Kpq_R	Kpq_R	q-axis PI controller proportional gain to be used in the inner PI controller
Tiq_R	Tiq_R	q-axis PI controller time constant to be used in the inner PI controller
KpQ_PCC	KpQ_PCC	q-axis PI controller proportional gain to be used in the PCC reactive power PI controller. Note that the order for this controller is iQCcmd provided by the IEC control blocks
TiQ_PCC	TiQ_PCC	q-axis PI controller time constant to be used in the PCC reactive power PI controller. Note that the order for this controller is iQCcmd provided by the IEC control blocks
<b>5. PLL control</b>		
Ki_PLL_DFIG	Ki_PLL_DFIG	Rotor side converter PLL integral gain
Kp_PLL_DFIG	Kp_PLL_DFIG	Rotor side converter PLL proportional gain
<b>6. AC voltage control</b>		
Vac regulator gain	Kp_Vac	AC voltage regulator gain
Vac regulator time constant	Ti_Vac	AC voltage regulator time constant
Vac max pu	1.1 [pu]	
Vac min pu	0.9 [pu]	

### 2.3.3 Detailed Converter Model

The detailed model consist of the two-level converters for both grid- and rotor-sides and is developed based on IGBT semiconductor switches as shown in Figure 19.

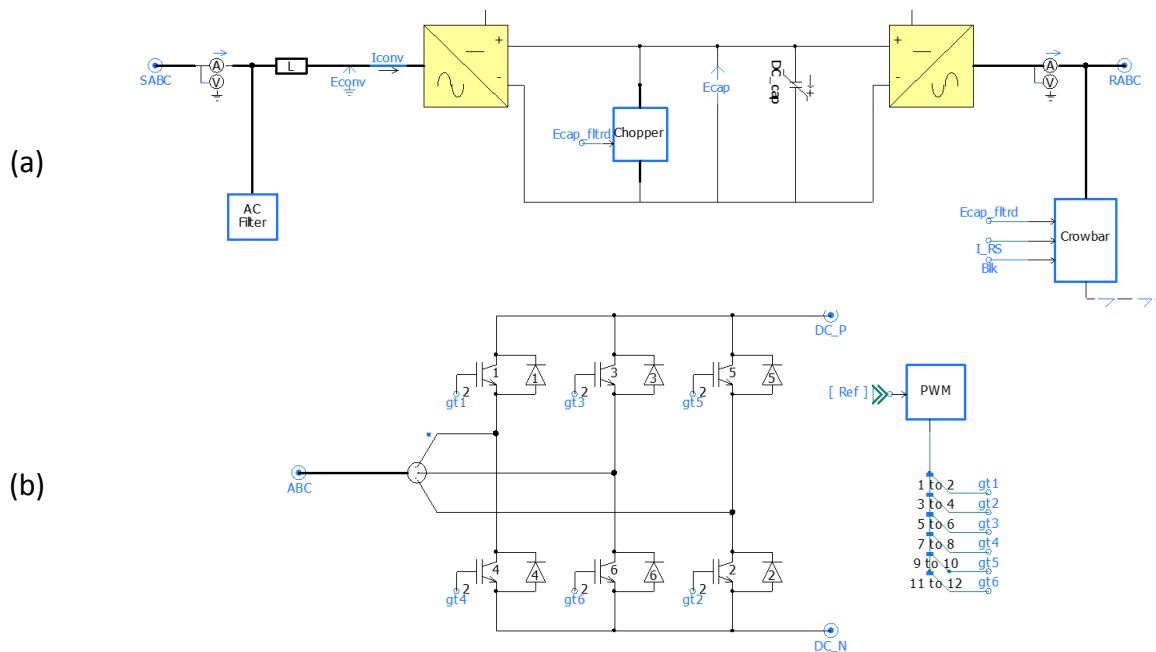


Figure 19: Detailed model: (a) AC-DC-AC converter, (b) two level converter used for both grid-side and rotor-side, (c) use layers to Enabled the detailed model and disabled average model

In this converter three-phase reference voltages are generated using sinusoidal pulse width (PWM) generation technique shown in Figure 20. In the case of the average model, the three-phase reference voltages are directly used by a set of three controlled voltage sources (one per phase) that replace the power electronic converters. Thus, lower simulation time step may be required to acceptable dynamics.

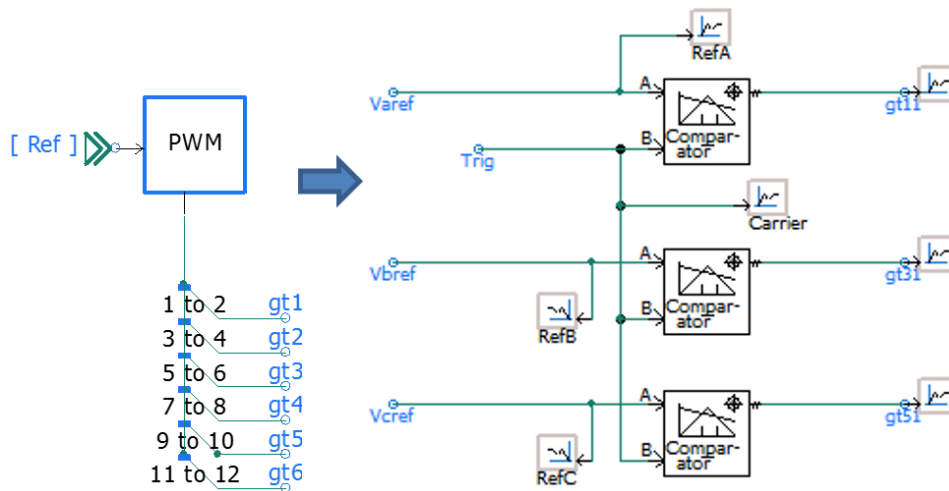


Figure 20: Sinusoidal PWM pulse generator

### 2.3.4 Average Converter Model

The average model of the converter shown in Figure 21 and can be used when focus of the simulation is not on the firing controls or on the effects of the harmonics produced by the power electronics converter.

In the average model, the AC side is interfaced with voltage sources set to generate the three-phase voltages references and on the DC side a current is injected such that the balance of power is preserved.

$$I_{dc}(t) = \frac{P_{ac\_measured}(t - \Delta t)}{V_{dc\_measured}(t - \Delta t)} \quad (5)$$

Note that:

1. One-time step delay is introduced in between the DC and AC circuits. For the most operation conditions this delay does not affect the results of the simulation.

- The diode bridge is to ensure that the balance of power and the accuracy of the simulation is preserved whenever the converter is blocked, as occurs before energization, or whenever the DC voltage drops below the peak AC voltage.

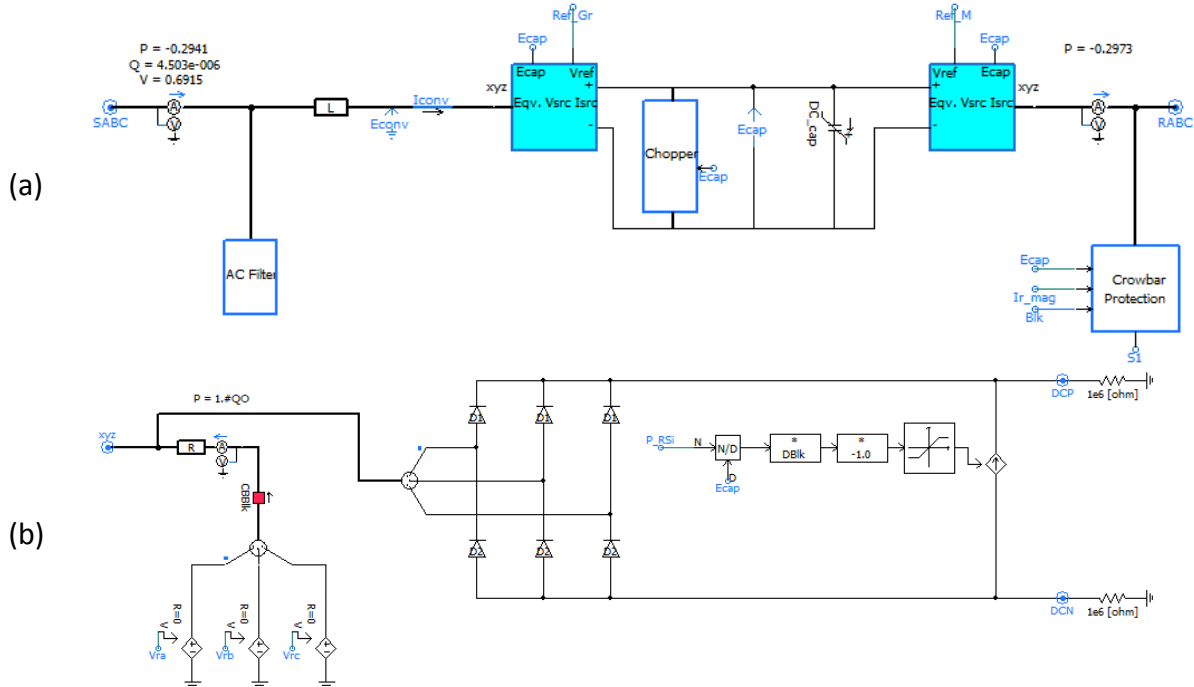


Figure 21: AC-DC-AC converter average model representation, (a) overall converter circuit, (b) the average circuit based on equivalent voltage source, (c) use layers to Enabled the average model and disabled detailed model.

The resistance 'R' is used to actuate the switching losses of the average model with the detailed model that has IGBT switches losses. Thus, it is selected to match the losses in the average and detailed models and achieve the same level of damping.

### 2.3.5 Grid-side controller

The grid-side control, shown in Figure 22, regulates the DC bus voltage (Ecap) and reactive power (Q). The reference for the reactive power control is set to zero.

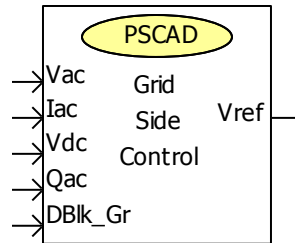


Figure 22: Grid-side control component

The grid-side converter parameters are given in Figure 23.

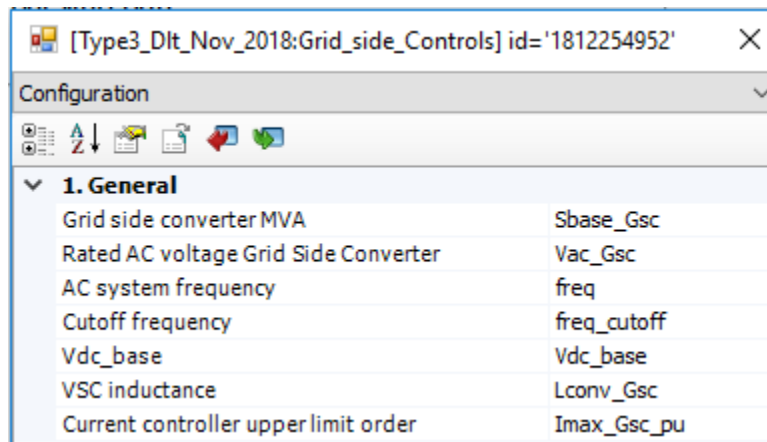


Figure 23: Grid-side control parameters

The per-unitization and transformation of current and voltage measurements are shown in Figure 24 and Figure 25 respectively. Low pass filters with characteristic frequency of 600 Hz were added to improve the quality of dq quantities by filtering out some of the high frequency harmonics of the power electronic converter.

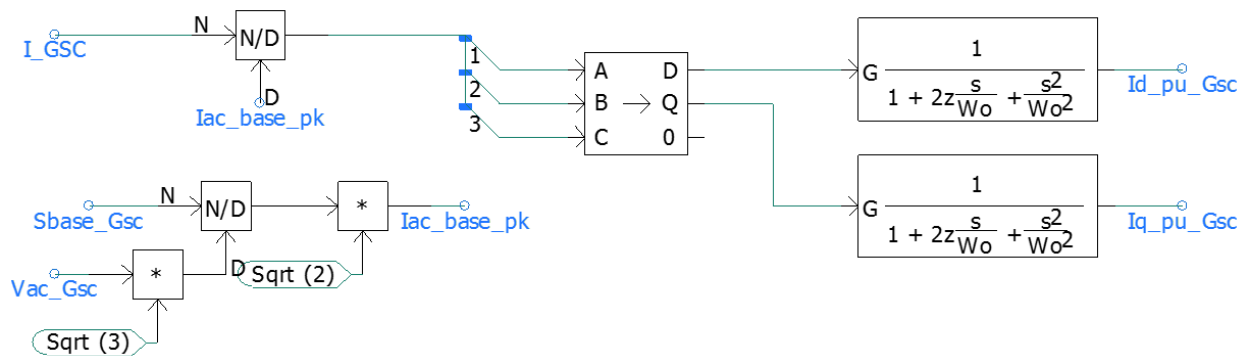


Figure 24: Current per-unitizing and transformation from abc to dq0

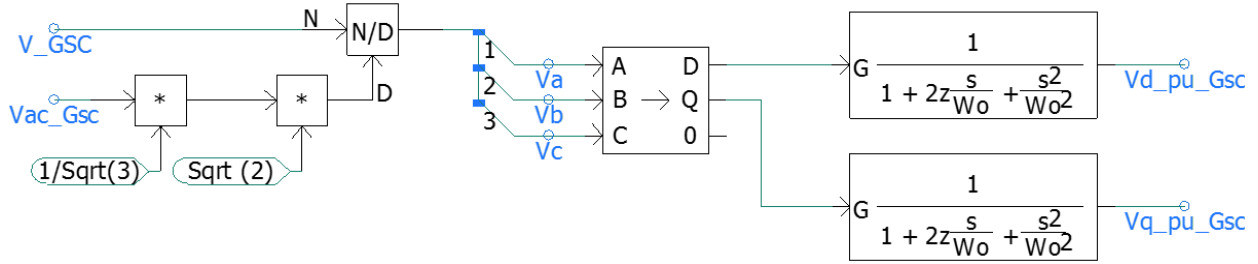


Figure 25: Voltage per-unitizing and transformation from abc to dq0

Base quantities for the grid-side converter controls and maximum converter currents are calculated based on the rated power ( $S_{base\_Gsc}$ ) and rated voltage ( $V_{ac\_Gsc}$  line to line, rms).

The DC bus voltage and reactive power controls are shown in Figure 26. These controllers generate the d-axis and the q-axis current orders (i.e.  $I_{d\_ord\_pu}$  and  $I_{q\_ord\_pu}$ ) for the decoupled control respectively. Normally this converter is operated such that no reactive power is transmitted to or absorbed from the AC system ( $Q_{ref} = 0.0$ ) at nominal voltage.

The current of the converter is limited by PI controller's limits. For this converter, the default limiting function is chosen to give priority to the d-axis as shown in Figure 27 (priority signal is set to 1). If the priority is given to the q-axis (Q control), the priority signal should be set to 0. The maximum Grid-side converter current rating has been set to 1.2pu to be able to work under low voltage ride trough.

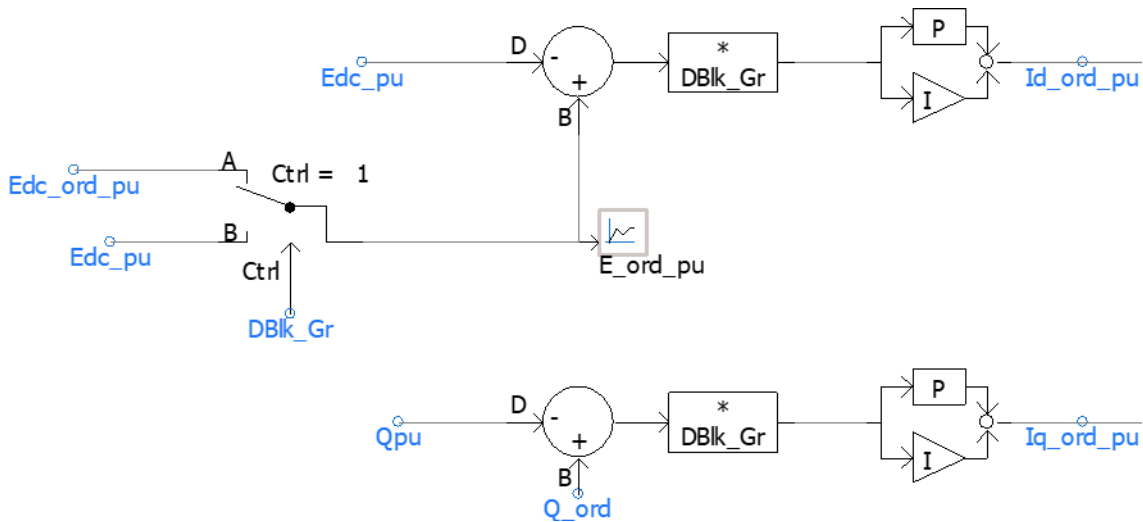


Figure 26: DC voltage and reactive power controllers

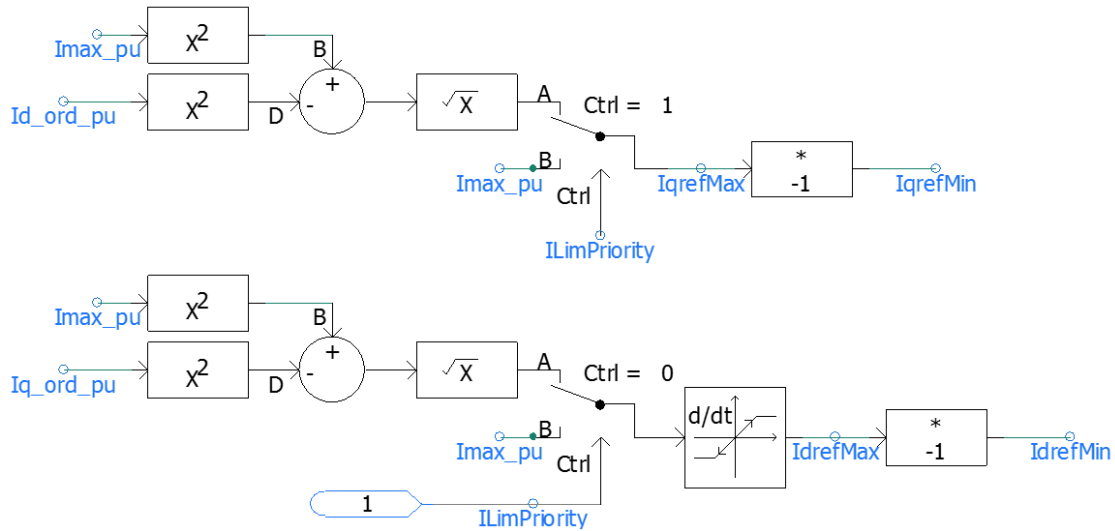


Figure 27: d- and q-frames current limit calculation

The decoupled current controls shown in Figure 28 are used to generate the converter reference voltages i.e.  $E_{d1ref}$  and  $E_{q1ref}$ . In order to decouple (i.e. reduce their effect on each other) the d and q frames the terms  $I_{q\_pu\_Gsc} * wL_{pu}$  and  $I_{d\_pu\_Gsc} * wL_{pu}$  are subtracted and added to d-frame and q-frame respectively.

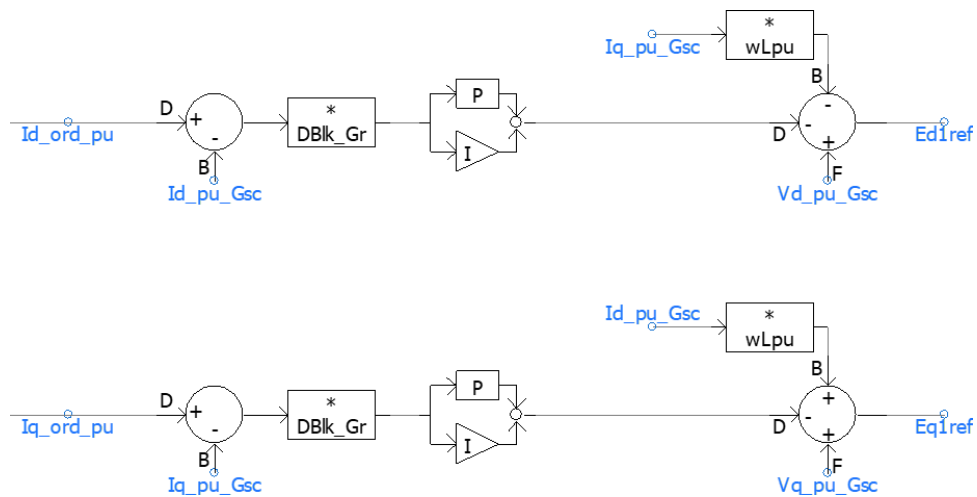


Figure 28: d- and q-frames decoupled current controllers

As shown in Figure 29, the reference voltages i.e.  $E_{d1ref}$  and  $E_{q1ref}$  are converted from rectangular to polar domain and the magnitude (M) is per unitized and limited to 1.15 pu. The three-phase reference voltage waveforms are obtained by applying the dq0 to abc transform to  $vd1_{ref}$  and  $vq1_{ref}$ , using thetaPLL as the conversion angle. Up to this point, the reference wave-



shapes are calculated in per-unit using the AC voltage peak to ground as the base voltage. These values need to be transferred to the adequate unit system depending on the type of model used. In the power electronics model, the base voltage of the reference wave shapes is changed from the converter AC voltage to the DC voltage.

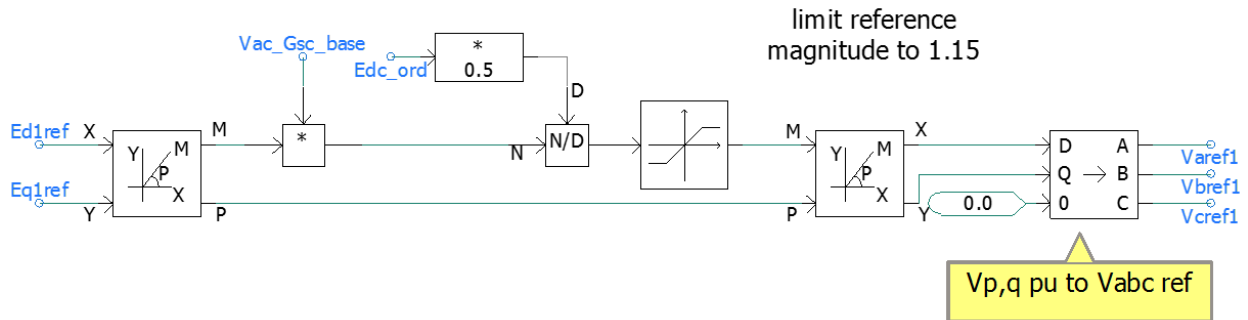


Figure 29: Reference voltages provided by grid-side controller

### 2.3.6 Rotor-side controller

The function of the rotor-side controller is to control active power (P) and reactive power (Q) (or AC voltage (Vac)) to obtain required ratings at the terminals of the wind turbine. The grid-side control is shown in Figure 30 .

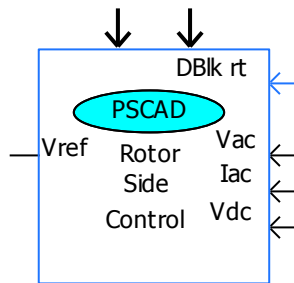


Figure 30: Rotor-side control component

The rotor-side converter parameters are given in Figure 23.

Configuration	
<b>1. General</b>	
System frequency	freq
DC nominal voltage [kV]	Vdc_base
Rotor-side converter rated MVA	Sbase_Rtr
Current controller upper limit order	Imax_Rsc_pu
Active power order	Pref_pu
<b>2. Machine data</b>	
Stator Resistance	Rst_pu
Machine terminal voltage	M_kv
Slip_max	Slip_max
Stator/Rotor Turns Ratio	TRN
<b>3. Low voltage active current management</b>	
Low voltage active current management (LVACM)	0.0
LVACM breakpoint high [pu]	0.8
Low voltage condition trigger voltage (pu)	0.9
High voltage condition trigger voltage (pu)	1.1
Terminal bus voltage filter time constant (s)	0.02

Figure 31: Rotor-side control parameters

The rated voltage of the rotor-side converter is calculated as follows (see reference [3] equation (15)):

$$V_{Rot} = \frac{M_{kv} \cdot Slip_{max}}{TRN} \quad (6)$$

Where Slip\_max, M\_kv, TRN are maximum slip, machine terminal voltage and stator/rotor turn ratio respectively.

To obtain the d and q components of the rotor current it is necessary to determine the relative difference between the stator flux and rotor position (slip angle). The position of the rotating flux is obtained via a phase lock loop (PLL) controller. As shown in Figure 32, the induced voltages of stator (Vst1\_a, Vst1\_b and Vst1\_c) are subtracted by the voltage drop across the stator resistance and then applied to the PLL controller. The rotor location (i.e. Theta) is generated by the induction

machine as the integral of the angular speed. In real world applications Theta might be generated by an actual position sensor.

The “Angle Resolver” component is to ensure that the angle generated is a ramp between 0 and  $2\pi$  range.

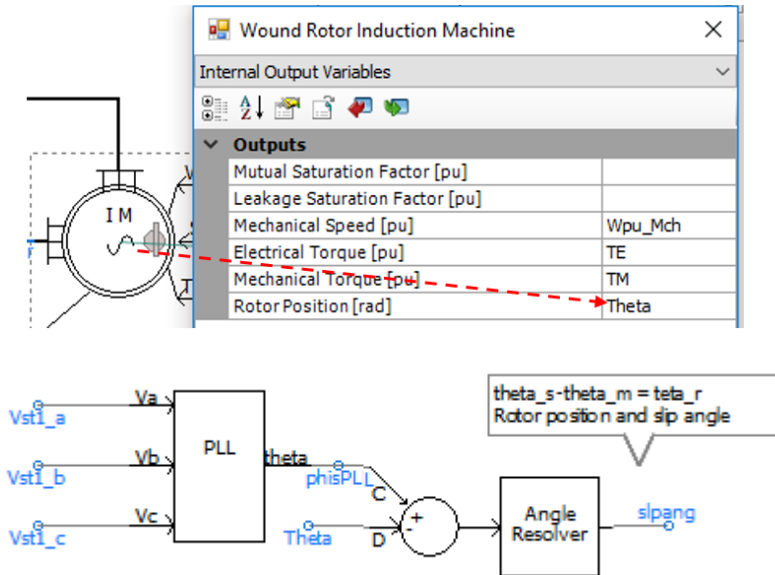


Figure 32: PLL controller to obtain the angle of d-q reference frame for rotor current. slpang is used to transform the d-q current frames to abc and vice versa

In this controller for simplicity the rotor angle is assumed to be placed in such a way that the d-axis flux in the air gap is aligned with d-axis of stator rotating flux, while the q-axis flux is aligned with the q-axis of stator rotating flux. Thus the  $i_d$  component contributes to the active power (or torque) generation, whereas the  $i_q$  component is contributes to the reactive power (AC voltage) generation.

The parameters for PLL controller are shown in Figure 33. The offset angle is selected equal to -1.57 rad (-90 degree) to align the d-axis flux of rotor in the air gap with d-axis of stator rotating flux, and the q-axis flux aligned with the q-axis of stator rotating flux.

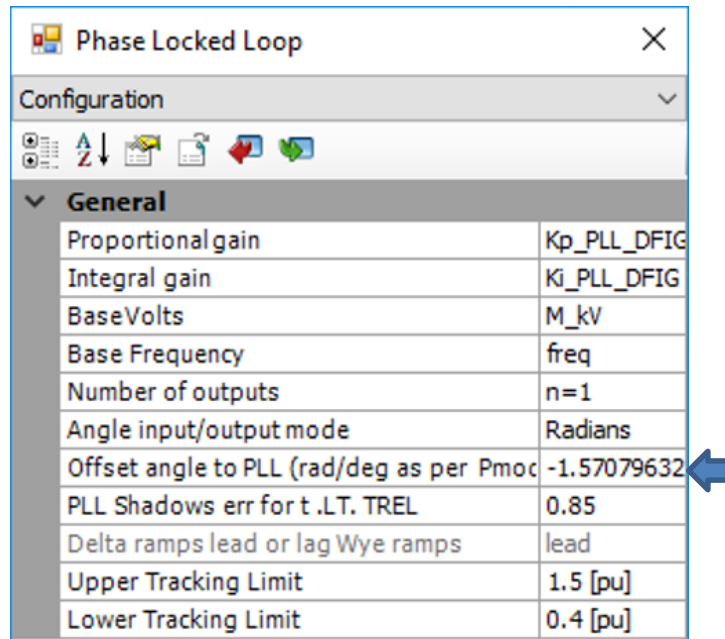


Figure 33: Rotor-side PLL parameters

Using the slip angle (slpang), the standard transformation block (ABC to dq0) can identify the d and q components of the rotor current, as shown in Figure 34.

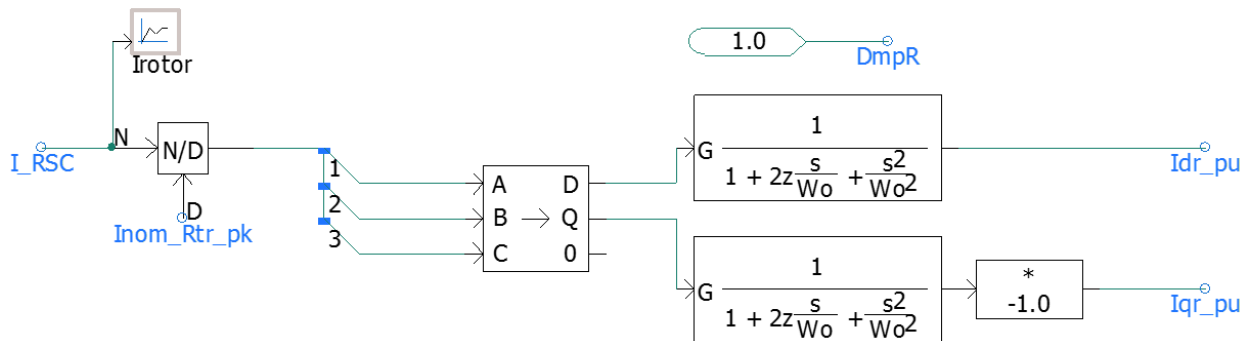


Figure 34: Rotor d and q axis components

The control circuits for the current and voltage components are represented in Figure 35. Once the induction machine is synchronized and the breaker closed, the loops for active and reactive power shown in Figure 35 come to operation. A soft transition between controllers is ensured by adjusting the PI controller limits.

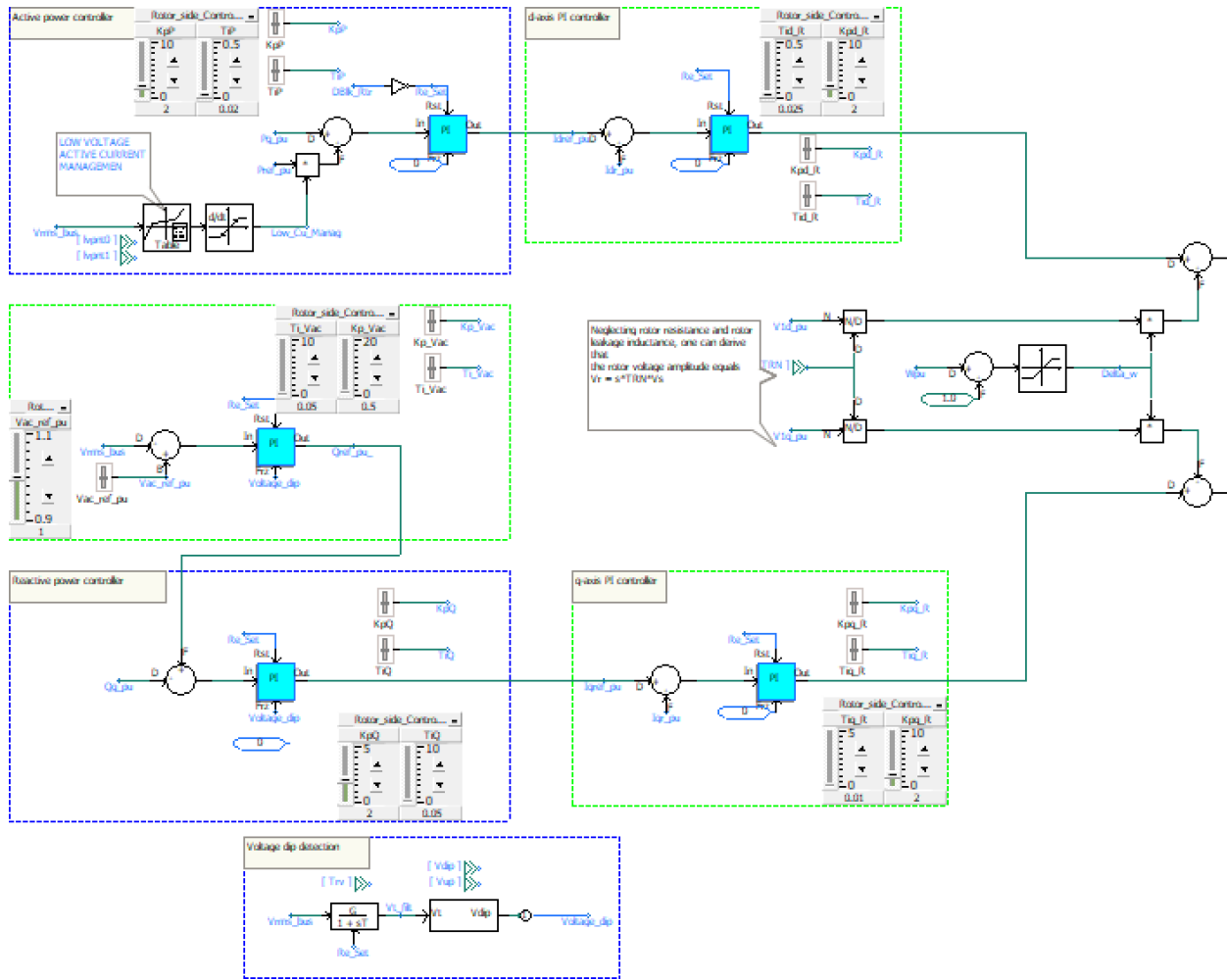


Figure 35: rotor-side active and reactive power controllers

## 2.4 Start-up Sequence of the Electrical System

The example provided here is designed to start on command. Therefore this model can be used when the AC voltage is not at steady state at the beginning of the simulation.

Figure 36 outlines the sequence of steps implemented in this example to start the wind generator. Note that this sequence is one of many methods that can be used to start-up a wind generators. For such purpose, the induction machine is started in speed control mode (input 'S'=1 in Figure 16 fixes machine speed to the value in input 'W' with the speed of the machine set to a preselected value  $\omega_0$  (e.g. 1.2 pu). Ideally this speed should be setup close to the final steady state rotating speed. In the default setup, the wind speed is assumed to be the rated wind speed  $\omega_0$  (e.g. 1.2 pu).

The start-up sequence is triggered upon closing of the AC breaker that links the wind generator with the AC system at the collector level voltage (normally 33 kV). The first converter to be de-blocked is the grid-side converter. This converter operates in DC voltage control. Once the DC voltage is achieved, the rotor-side converter is de-blocked. The function of this converter at this stage is to inject currents into the machine rotor windings, such that an AC voltage that matches the AC grid-side voltage at the 0.9 kV bus is established.

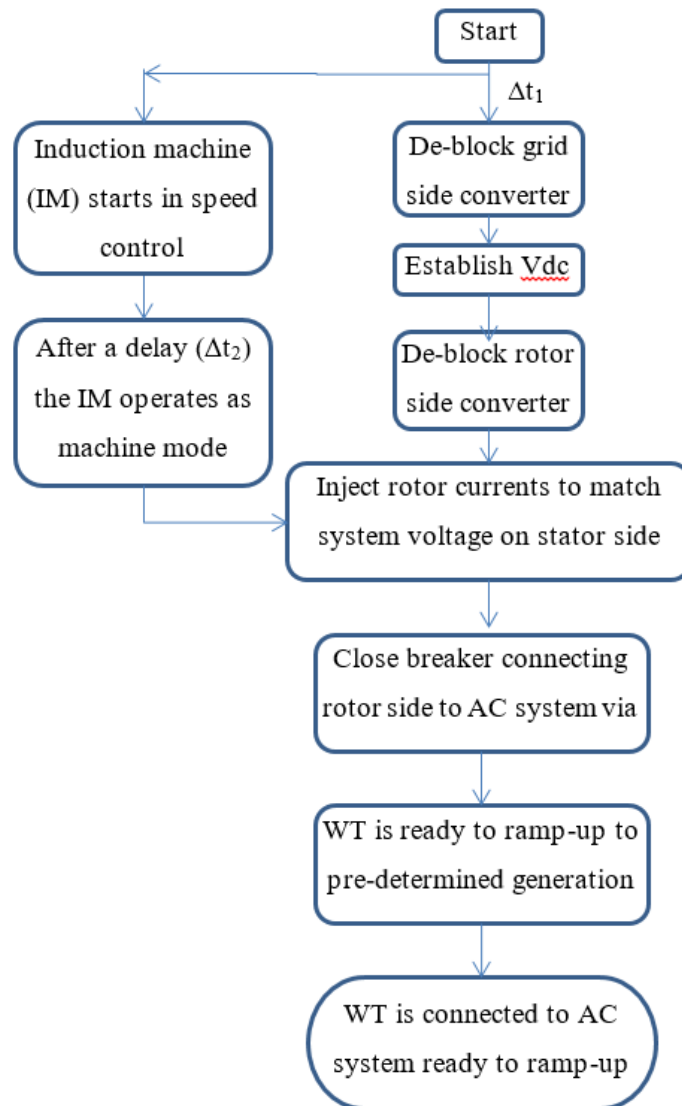


Figure 36: Start-up sequence of the electrical system

When the magnitude and phase of voltage on the stator (Vst1) is matched with the magnitude of the grid voltage (Vst2), a synchronizer control (described in next section) closes the stator side breaker, connecting the induction generator to the grid.

At this point the rotor-side converter changes control mode to P and AC voltage control mode and the machine is ready to start transferring mechanical power to the grid. The implementation of the start-up sequence is presented in Figure 37.

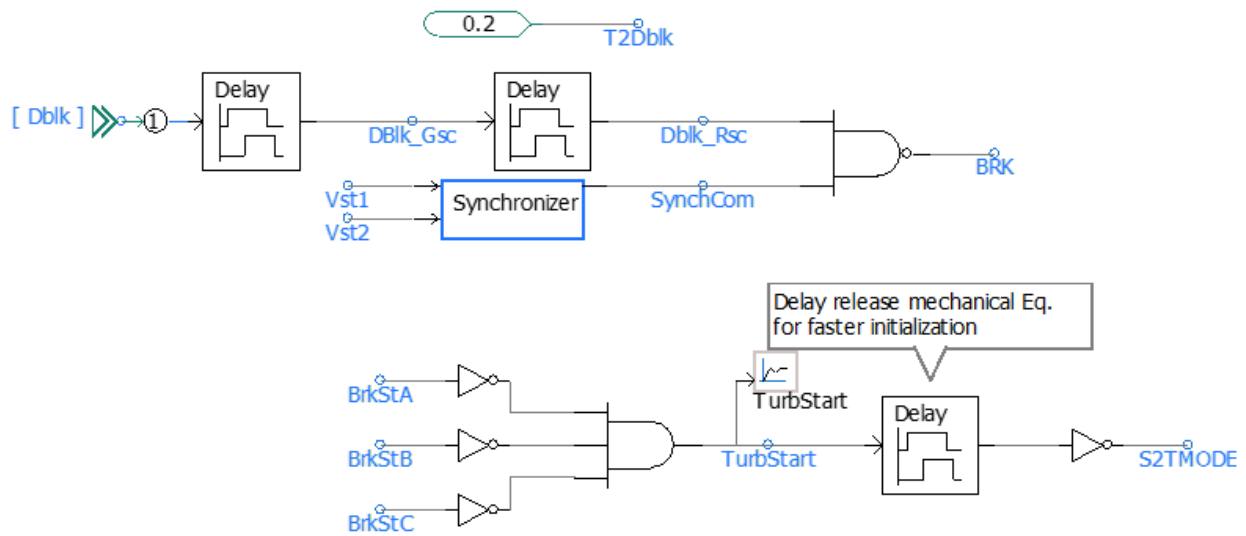


Figure 37: Implemented logic for start up

### 2.4.1 Synchronization

Synchronization is based on a simplified algorithm that only checks the instantaneous value of the voltage magnitude ( $\Delta V$ ) of the both side of the breaker. In this example, ( $\Delta V$ ) is selected equal to 0.2pu. The parameters for the synchronizer block are shown in Figure 38.

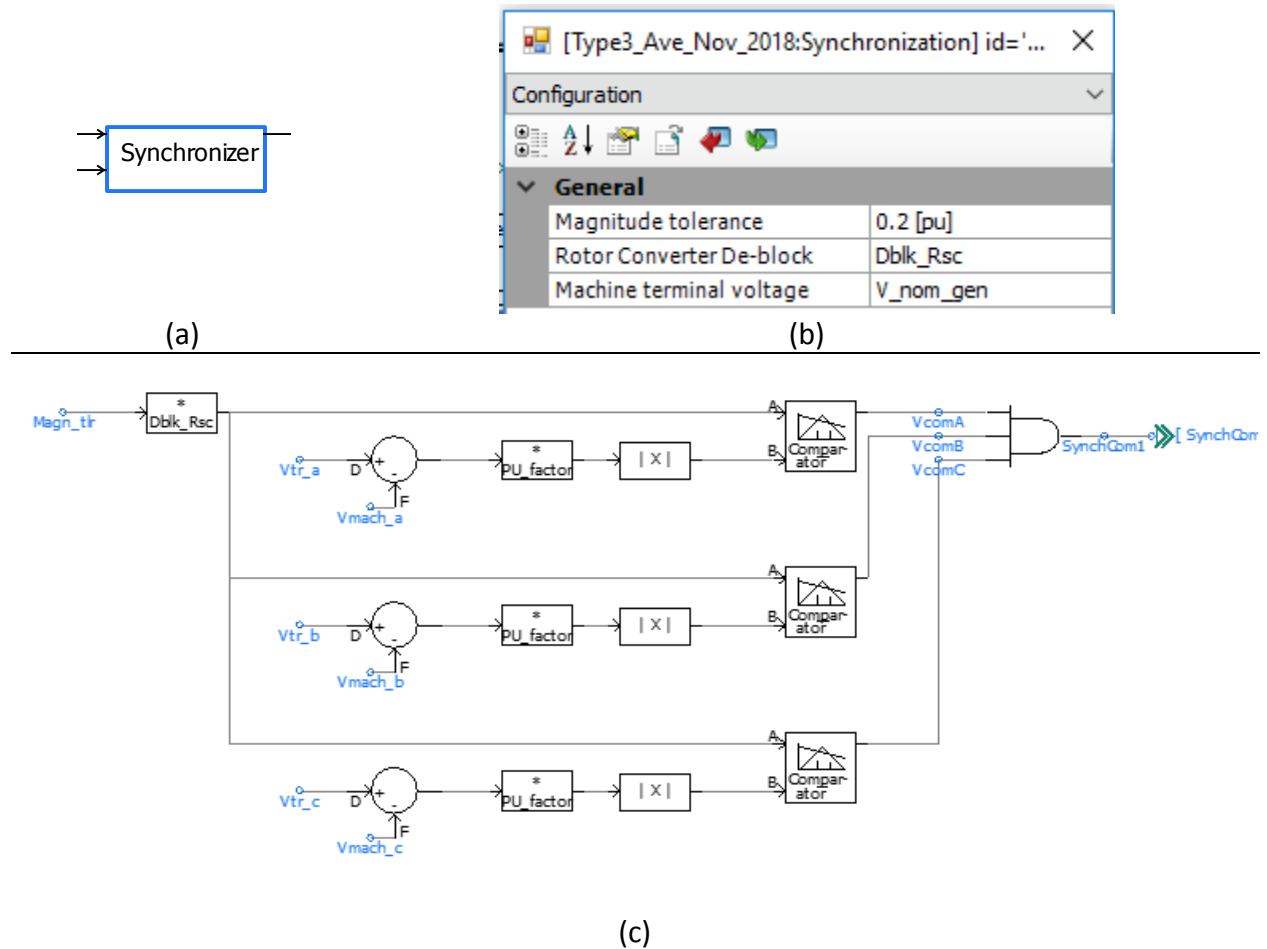


Figure 38: synchronizer module (a) component; (b) component, (b) Parameters, (c) logic of synchronization

## 2.5 Crowbar Protection

According to most new grid code requirements, wind turbines must remain connected to the grid during grid disturbances and provide voltage support during and after the faults [1]. The crowbar system is essential to avoid disconnection of wind turbine from network during the fault. Moreover, the insertion of the crowbar in the rotor circuits enables a more efficient voltage control during faulty conditions.

As wind turbine based on DFIG has the stator connected to the grid, it makes the rotor winding sensitive to high currents induced during faults. Also the rotor windings are connected to the grid via AC-DC-AC converter, which is very sensitive to over-currents. The most common means to

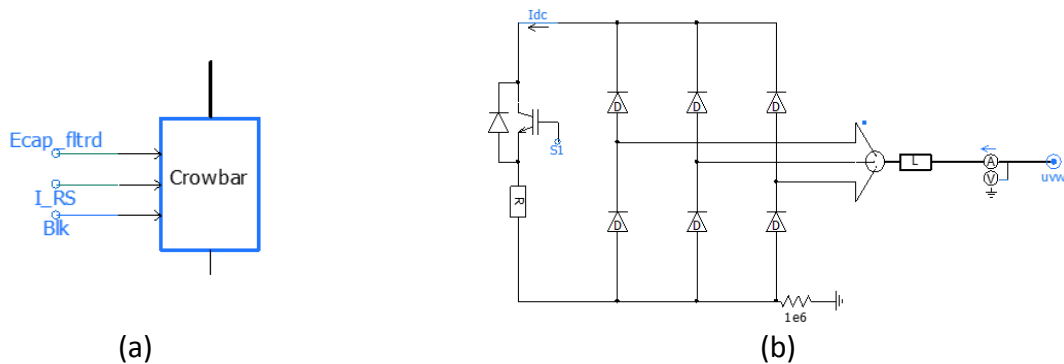


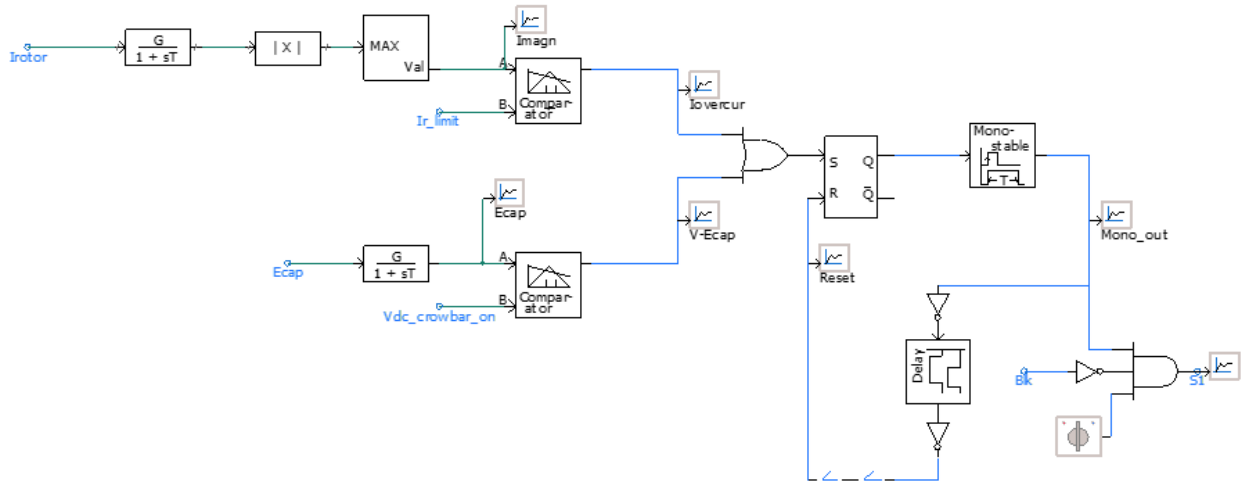
avoid injecting high currents into the power electronic converters is to short circuit the rotor terminals via a resistance. Such mechanism is normally known as crowbar.

The duration of the crowbar activation depends on grid requirements. For grids with low wind penetration the injection of reactive current during the faults is not required normally. In this case the crowbar is usually activated for whole duration of the fault.

However, during crowbar protection the wind turbine cannot inject reactive power. Therefore crowbar protection is activated for a fixed time period e.g. 50 to 100 ms. The philosophy behind this is that the highest induced currents in the rotor circuit happen in the first two cycles after the inception of the AC fault. Under this scheme, the crowbar is enabled for the few first cycles after inception of the fault, to protect the converter from high magnitude fault currents injected into rotor and it is disabled to allow the converter inject reactive power into the grid and support low voltage ride through. In the example, the crowbar is activated for a period of 60 ms.

The crowbar system is a resistance controlled by power electronics. In the DFIG files provided, two different options were provided for the activation of the crowbar system, the DC voltage exceeding a predetermined DC voltage, or the rotor currents exceeding a predetermined value. The logic behind the crowbar control is illustrated in Figure 39.



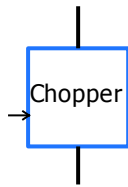


(c)

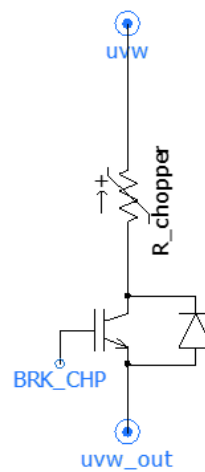
Figure 39: Crowbar protection (a) power electrical circuit (c) logic

## 2.6 DC-link Chopper

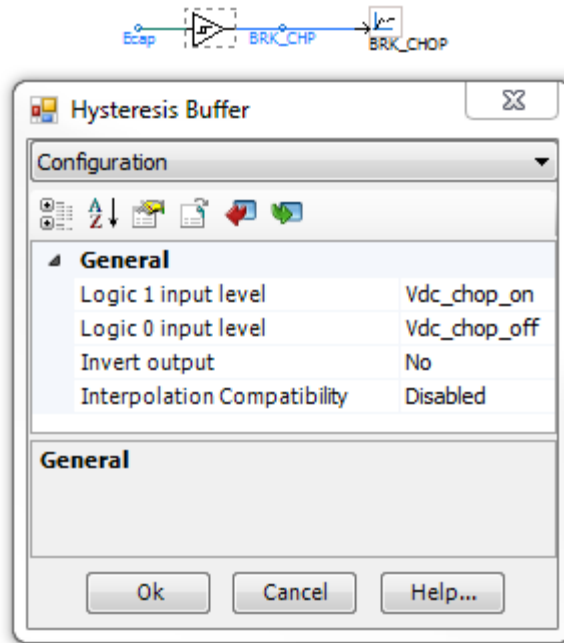
Further protection during fault condition is required to avoid overvoltage on the DC-link capacitor. This protection is provided by the DC-link Chopper which is IGBT-controlled resistance that dissipate overvoltage. A voltage hysteresis controller is used to issue the chopper firing pulses. The logic of the DC-link Chopper is illustrated in Figure 40.



(a)



(b)



(c)

Figure 40: DC-link chopper (a) component, (b) electrical circuit (c) hysteresis controller

## 2.7 Low Pass Filter

The power electronic converters generate a considerable amount of harmonics. A filter is used on the grid side to minimize the impact of harmonics on the grid. The structure of the filter is represented in Figure 41. There are several filter topologies and methods suggested in the literature on how to calculate the filter parameters.

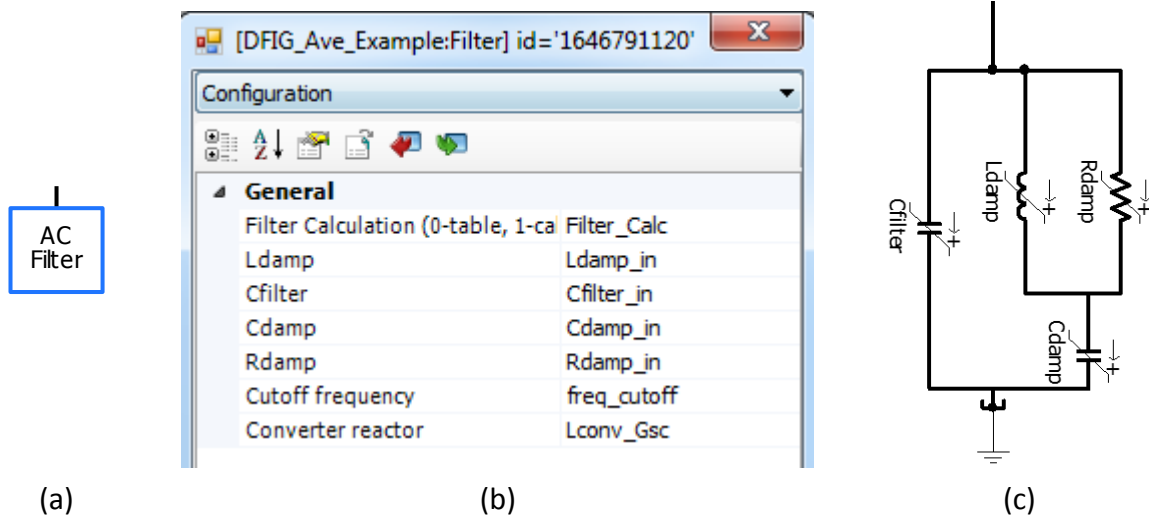


Figure 41: AC filter (a) AC filter component (b) the parameters (c) circuit

### 2.7.1 Filter parameters calculation

The methodology used in this example to calculate the filter parameters is demonstrated in this section. According to [1], the switching frequency can be calculated as follows

$$f_{sw} = \frac{V_{DC}}{8 \times L_{inv} \times I_{rpp}}, \text{ where} \tag{9}$$

$I_{rpp}$  – the peak-to-peak amplitude of the ripple current, which can be estimated as 20% of peak-to-peak nominal current:

$$I_{maxAC} = I_{nomAC} \times \sqrt{2} \quad , \text{ where} \tag{10}$$

$$I_{nomAC} = \frac{P_{conv}}{\sqrt{3} \times V_{L-Lrms}} \tag{11}$$

For our system using (10) and (11) the peak-to-peak current will be

$$I_{nomAC} = \frac{2.14}{\sqrt{3} \times 0.69} = 1.79 \text{ kA}$$

$$I_{maxAC} = 1.79 \times \sqrt{2} = 2.54 \text{ kA}$$

The ripple current approximately

$$I_{rpp} = 0.2 * 2.54 = 0.508 \text{ kA}$$

The switching frequency using (9)

$$f_{sw} = \frac{1.45}{8 \times 0.000106 \times 0.508} = 3369 \text{ Hz}$$

The carrier frequency as multiple of fundamental:

$$C_{freq} = \frac{f_{sw}}{f} \quad (12)$$

$$C_{freq} = \frac{3369}{50} = 67.38$$

A cutoff frequency of 200 Hz for the filter is used.

The filter capacitance needed to provide the cutoff frequency with the inductor (L) can be found as follows:

$$C_{filter} = \frac{1}{(2 \times \pi \times f_{cutoff})^2 \times L} \quad (13)$$

The filter capacitance for the system using (A5)

$$C_{filter} = \frac{1}{(2 \times \pi \times 200)^2 \times 0.000106} \times 10^6 = 5974 \text{ uF}$$

The damping circuit is needed to reduce or eliminate any possible ringing caused by the combination L and  $C_{filter}$ . The damping inductance takes the value of:

$$L_{damp} = 5 * L_{VSC} \quad (14)$$

$$L_{damp} = 5 * 0.000106 = 0.00053 \text{ H}$$

The damping capacitance can be calculated:

$$C_{damp} = \frac{C_{filter}}{2} \quad (15)$$

$$C_{damp} = \frac{5974}{2} = 2987 \text{ uF}$$

The damping resistance can be calculated:

$$R_{damp} = \sqrt{\frac{L_{damp}}{C_{damp}}} \tag{16}$$

$$R_{damp} = \sqrt{\frac{0.00053}{0.002987}} = 0.4212 \Omega$$

### 2.8 Scaling Component

Figure 42 shows the scaling component that represents an aggregated wind farm. In this example the wind farm has 100 units. The output current of the wind turbine is multiplied by the number of units ( $n = 100$ ) and injected to the power system through current sources.

Also the scaling component should be considered when it comes to reactive power. The scaling component is modelled similar to a transmission line with one simulation time step ( $dt$ ) delay. The equivalent capacitor ( $C$ ) value can be calculated for this component in (7):

$$C = dt/Z_c \tag{7}$$

where  $dt$ , and  $Z_c$  are simulation time step and the equivalent surge impedance, respectively.

The equivalent surge impedance can be calculated as (8) :

$$Z_c = \sqrt{L/C} \tag{8}$$

To minimize the effect of the series inductor of the scaling component we can use part of leakage reactance of the connecting transformer or interconnected cables and transmission lines if there is any. A damping resistance may use in parallel to this component to damp numerical instability.

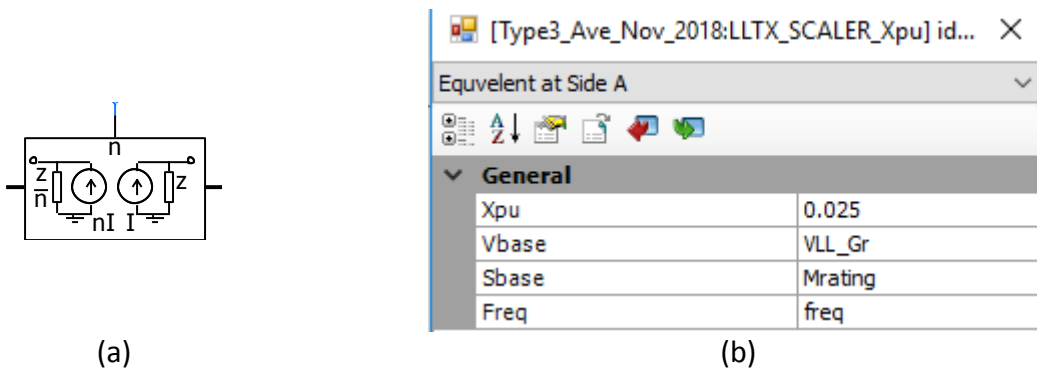


Figure 42: Scaling component to aggregate wind farm (a) the component (b) the input parameters

### 3 Dynamic responses of the detailed and the average models

The dynamic behaviors of the detailed and average models are compared during two transient conditions. In the first transient the wind speed is varied slowly around its nominal speed to obtain lower and higher speed ratings. In the second transient a three phase to ground fault is incepted on the Bus1 for duration of 0.15sec.

#### 3.1 Dynamics against wind speed variations

Figure 43 and Figure 44 show dynamic responses of the average and detailed models respectively when the speed of wind is changes over time. It can be seen that the dynamics of the average and detailed models are quite similar and close enough to use averaged model as a replacement of the detailed model. Also, total CPU Time for average model is 515.172 s while it is about 1105.5S for detailed model. This indicates that, the average model is almost 2 times faster than the detailed model in terms of simulation time.

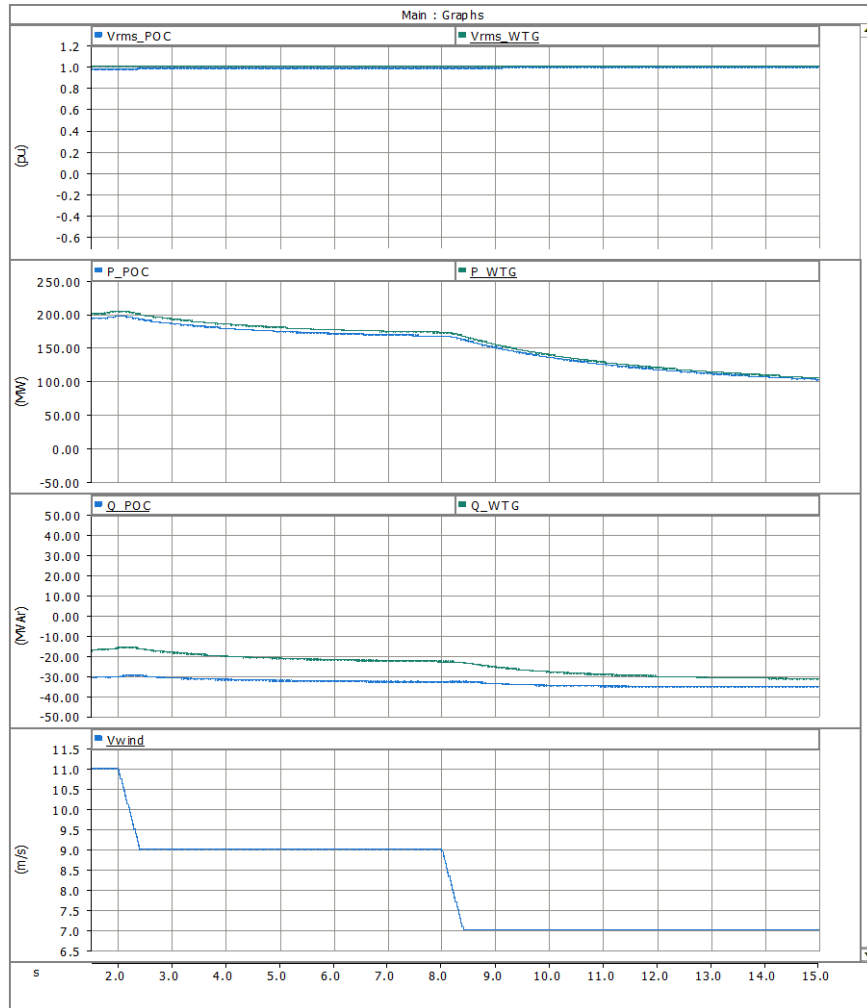


Figure 43: Dynamic responses of the average model during a change in a wide range of wind speed



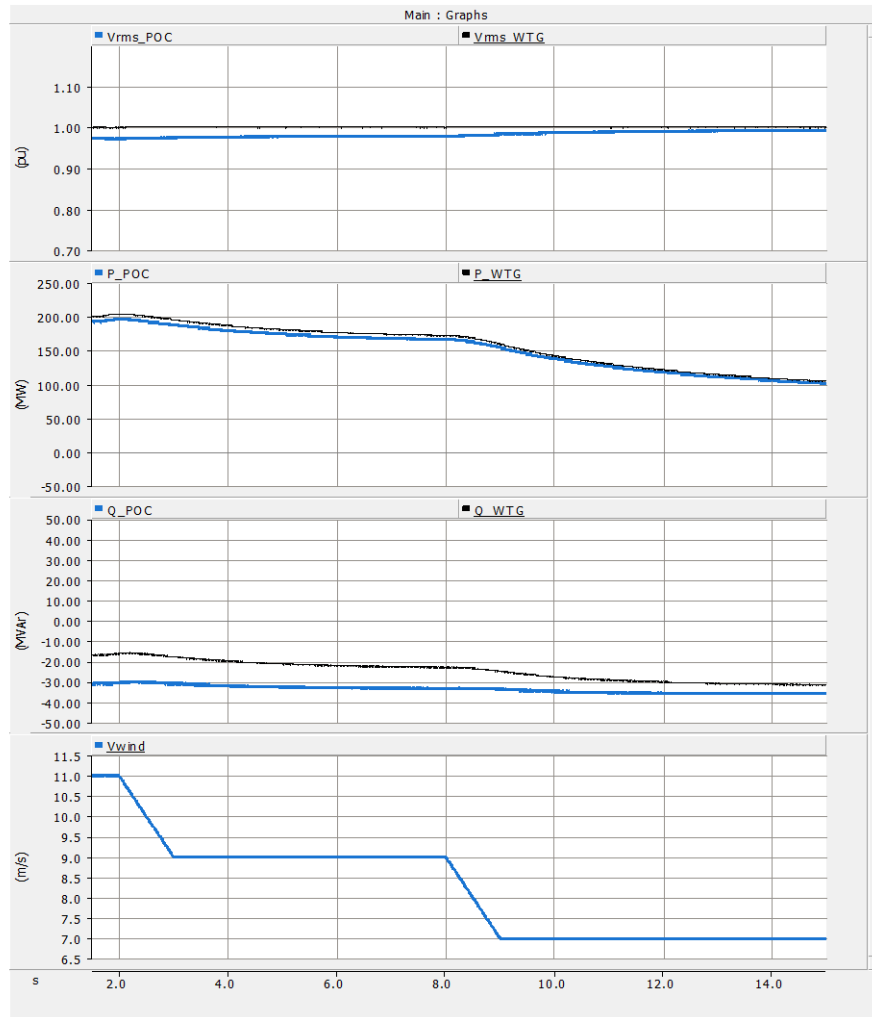


Figure 44: Dynamic responses of the detailed model during a change in a wide range of wind speed

### 3.2 Dynamics against faulty condition

Figure 45 and Figure 46 show the dynamic responses of the average and detailed models during a three phase to ground fault on the Bus1 at 7sec respectively. As it is expected both the models inject same amount of reactive power (20MVar) to the grid and the active power increases slowly to its nominal value (200MW).

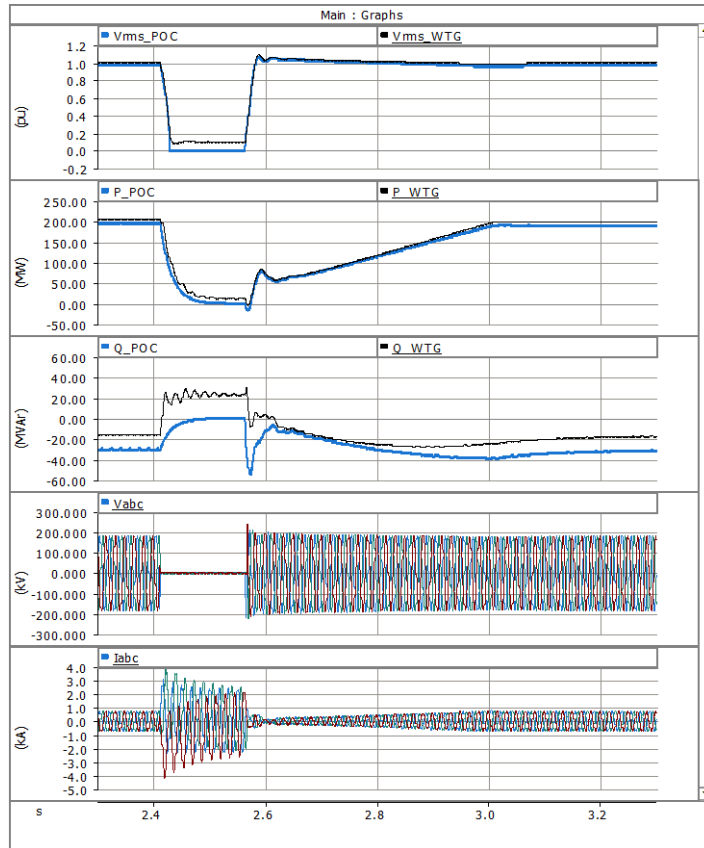


Figure 45: Dynamic responses of the average model for a fault on POC

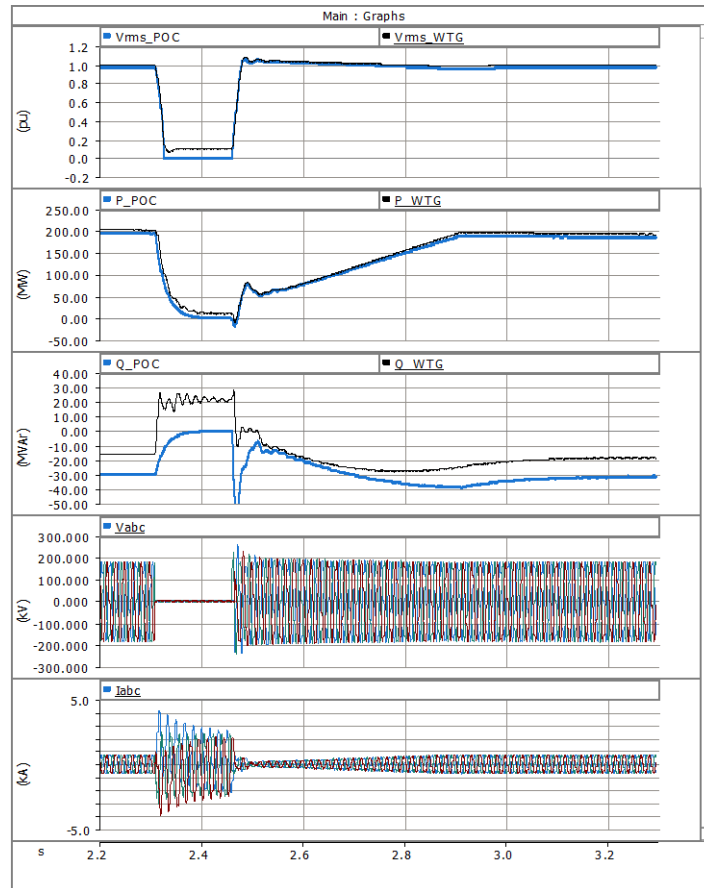


Figure 46: Dynamic responses of the detailed model for a fault on POC

## 4 References

- [1] A. Y. Goharrizi, J. C. Garcia Alonso, E. Borisova, F. Mosallat and D. Muthumuni, "Benchmark Model of Type-III Wind Turbine for Research and Development Applications," 2018 IEEE Canadian Conference on Electrical & Computer Engineering (CCECE), Quebec City, QC, 2018, pp. 1-6.
- [2] Kara Clark, Nicholas W. Miller, Juan J. Sanchez-Gasca, "Modeling of GE Wind Turbine-Generators for Grid Studies," Version 4.5, April 16, 2010
- [3] S. Muller, M. Deicke, and R. D. Doncker, "Doubly fed induction generator systems for wind turbines," IEEE Industry Applications Magazine, vol. 8, pp. 26–33, June 2002. (15)
- [4] R. Pena J.C. Clare G. M. Asher "Doubly fed induction generator using back-to-back PWM converters and its application to variable speed wind-energy generation" IEE Puoc.-Electr. Power Appl. Vol. 143 No 3 May 1996. (16)